The Location of the Neutral Axis in Wood Beams with Multiple Knots

An Abstract of the Thesis of

Levi R. Voigt for the degree of Honors Baccalaureate of Science in Civil Engineering presented May 31, 2011. Title: The Location of the Neutral Axis in Wood Beams with Multiple Knots.

Abstract Approved: ______________________________

Rakesh Gupta

____

Thomas H. Miller

In a homogenous and isotropic material, the location of the neutral axis coincides with the location of the centroid of the beam. Wood is anisotropic, meaning that it has different properties in different directions. It is also non-homogenous, meaning that the beam exhibits different properties at different locations throughout its length due to the presence of knots as well as grain characteristics. Since wood is not homogenous or isotropic, the location of the neutral axis varies throughout the length of the beam and is different for each individual beam. Because of this variability, research is needed to better understand the movement of the neutral axis as it reacts to different combinations of knots and grain angles. This thesis explores this in 38 mm by 89 mm (nominal 2X4) Douglas Fir beams with different patterns of knots. The analysis was done using Digital Image Correlation equipment and VIC-3D software which displays the strains and thus the location of the neutral axis. It was found in a clear nominal 2 in x 4 in beam that the neutral axis was slightly above the center of the beam. In the beams containing knots, the location of the neutral axis tended to move away from the knots except in situations where the knots were located longitudinally close to each other. In this case, the neutral axis moved very minimally or not at all.

Key Words: Isotropic, Homogenous, Neutral Axis, Wood Beams, Knots
Corresponding e-mail address: voigtl@onid.orst.edu

The Location of the Neutral Axis in Wood Beams with Multiple Knots

The Location of the Neutral Axis in Wood Beams with Multiple Knots

The Location of the Neutral Axis in Wood Beams with Multiple Knots

By

Levi R. Voigt

A PROJECT

Submitted to

Oregon State University

University Honors College

In Partial Fulfillment of the

Requirements for the degree of

Honors Baccalaureate of Science in Civil Engineering

Presented May 31, 2011

Commencement June 11, 2011

The Location of the Neutral Axis in Wood Beams with Multiple Knots

Honors Baccalaureate of Science in Civil Engineering project of Levi R. Voigt presented on May 31, 2011.

APPROVED:

Thomas H. Miller, PhD, PE
Mentor, representing Civil Engineering

Rakesh Gupta, PhD
Mentor, representing Wood Science and Engineering

Milo Clauson
Committee Member, representing Wood Science and Engineering

Head, School of Civil and Construction Engineering

Dean, University Honors College

I understand that my project will become part of the permanent collection of Oregon State University, University Honors College. My signature below authorizes release of my project to any reader upon request.

Levi R. Voigt, Author

ACKNOWLEDGMENTS

This thesis can be greatly accredited to the dedication and devotion of my co-mentors, Thomas Miller, Associate Professor in Civil and Construction Engineering and Rakesh Gupta, Professor in Wood Science and Engineering at Oregon State University. I would also like to send a special thanks to my committee member, Milo Clauson, a Senior Faculty Research Assistant in Wood Science and Engineering. Without the help of these outstanding Oregon State University faculty members, the completion of this thesis would not have been possible.

The Location of the Neutral Axis in Wood Beams with Multiple Knots

Table of Contents

Page

List of Figures

List of tables

Table **Page**

List of Appendices

Appendix Page

1.0 INTRODUCTION

When a beam is subjected to bending, the top half of fibers are in compression and the bottom half of fibers are in tension. The neutral axis in any beam is defined as the point near the middle of the beam where the compression zone and the tension zone meet and the resulting longitudinal; strains and, therefore, stresses are zero. A simple diagram can be drawn to show this distribution of stresses as they vary throughout the depth (D) of the beam. This diagram is shown in Figure 1.1.

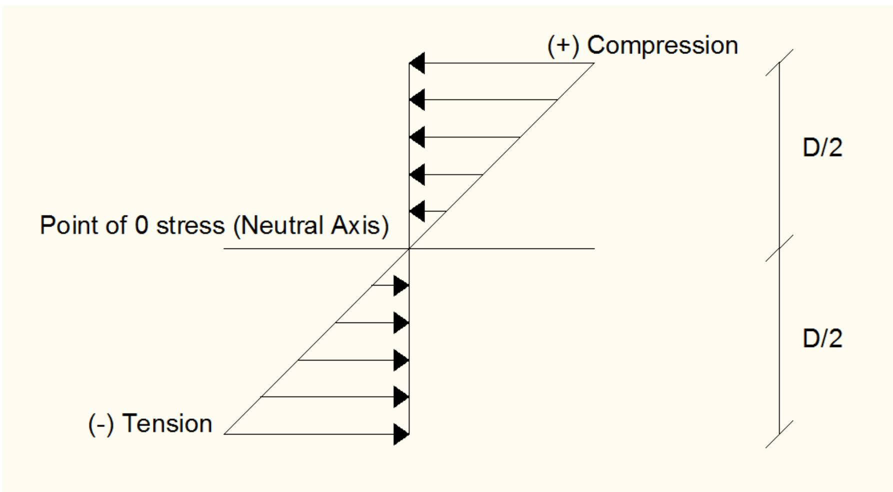

Figure 1.1: Location of the Neutral Axis in an isotropic and homogeneous beam

In beams that are made of a homogenous and isotropic material, the modulus of elasticity in all sections of the beam is equal and the resulting location of the neutral axis will coincide with the location of the centroid of the beam. However, wood is a non-homogenous, anisotropic material, meaning that it exhibits different properties in different directions and also in different portions of the beam. Therefore, an analysis will need to be done to explore how the location of the neutral axis responds to the presence of different knots in different locations for individual beams. The focus of this thesis will be on the effects of the presence of multiple knots located in the compression zone, tension zone, and center of the beam.

1.1 Objectives

This thesis will be an extension of two theses written by former students of the Oregon State University Honors College. The first thesis on this topic was done by Sarah Holm (2007). In her thesis, Holm examined the location of the neutral axis in 1 in x 1 in Douglas Fir beams with single knots located in the compression zone, the tension zone, and the center of the beam. She also examined the location of the neutral axis in a 1 in x 1 in clear beam. Davis (2010) expanded upon this research by setting up an experiment that explored the differences in the neutral axis location for different species of 1 in x 1 in wood beams, as well as testing different specimens of Douglas Fir nominal 2 in x 4 in beams. Of the 2 x 4 beams, one was a clear beam containing no knots, one had a knot in compression, one a knot in tension, and one a knot in the center of the beam. My research will further expand the previous research done by exploring the effects of multiple knots in 2 x 4 Douglas Fir beams. The specimens used in this experiment contained different combinations of knots located in the tension zone, compression zone, and center of the beam. It was attempted to find pairs of beams that contained a similar pattern of these knots. Having pairs with similar characteristics would likely produce similar strain patterns and, therefore, aid in drawing conclusions concerning the location of the neutral axis of wood beams containing multiple knots.

1.2 Personnel

This project was conducted by Levi R. Voigt, an undergraduate student in Civil Engineering in the University Honors College at Oregon State University, under the supervision of Dr. Thomas Miller, Associate Professor of Civil Engineering at Oregon State University and Dr. Rakesh Gupta, Associate Professor of Wood Science and Engineering at Oregon State University. The testing was done with the help of a Senior Faculty Research Assistant in the Wood Science and Engineering Department at Oregon State University, Milo Clauson, and also Dr. Lech Muszynski, a Professor in the Wood Science and Engineering Department at Oregon State University. Milo Clauson also contributed to a discussion which resulted in my understanding of how to interpret and analyze the data.

2.0 Literature Review

2.1 Elastic Behavior of Beams

When a beam is subjected to bending with downward loading, the top of the beam will experience compression strains and the bottom will experience tensile strains. These strains will result in longitudinal stresses in the beam. The strain in the compression zone will shorten the beam while the strain in the tension zone will lengthen the beam. This behavior can be seen in Figure 1.1.

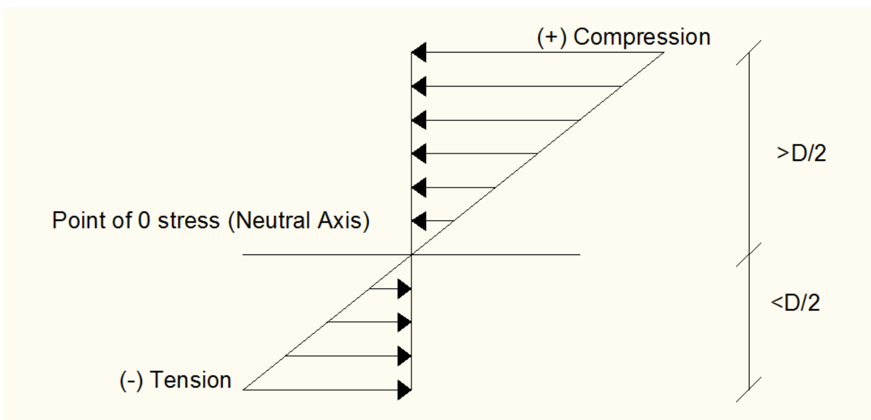

Figure 2.1: A portion of the beam will experience compression stress and a portion will experience tensile stress. In this rectangular beam, the material is anisotropic and non-homogenous so the maximum compression stresses and tension stresses are not equal (Gere and Timoshenko, 1997).

Kollman and Cote (1968) explain that when a beam is elastic, it has not been subjected to any stresses greater than the yield point. The yield stress is the point where the stress-strain curve begins to flatten out, and the material has a greater strain for each added unit of stress. When a material is subjected to stresses less than the yield stress of that particular material, it will return to its original shape when the stresses are removed; thus behaving elastically. Stress-strain curves for small wood beams in compression and tension are shown in Figure 2.2.

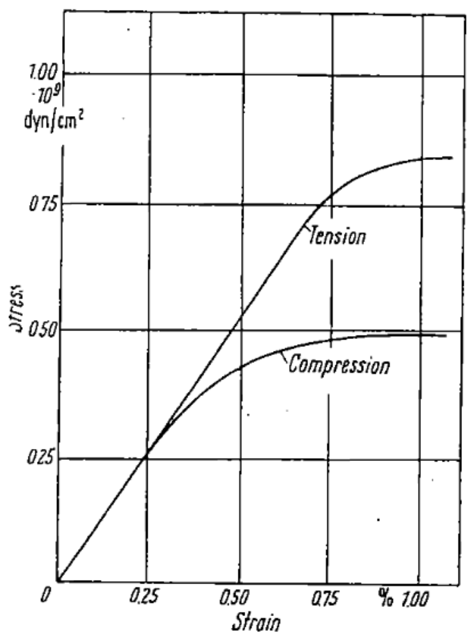

Figure 2.2: Typical Stress-Strain Curve for small wood beams (Kollman and Cote, 1968)

When observing the stress-strain curves for both compression and tension, it is clear that the yield stress in compression is much lower than the yield stress in tension. Since this is the case for clear wood beams, as the beam approaches its ultimate strength, the compression zone will become slightly larger and the tension zone will become smaller, and the neutral axis will be forced further toward the bottom of the beam to accommodate for the smaller modulus of elasticity in compression. This was shown by both Davis (2010) and Holm (2007) in the testing of 1 in x 1 in clear wood beams. This movement of the neutral axis was also shown in a study done by Heather Redler (Redler, 2006).

2.2 Inelastic Behavior of Beams

Elastic behavior was explained in the previous section and in this section we will explore inelastic material behaving. Inelastic behavior occurs when the stresses applied to the material exceed the yield stress. When a stress greater than the yield stress is experienced, the beam will not return to its original shape when the stress is removed. Using the stress distribution shown in Figure 2.1, we can see that the largest stresses occur at the extreme fibers at the top and bottom of the beam. When a beam begins to yield, the stress distribution will progress as shown in Figure 2.3 (Bažant and Jirásek 2002).

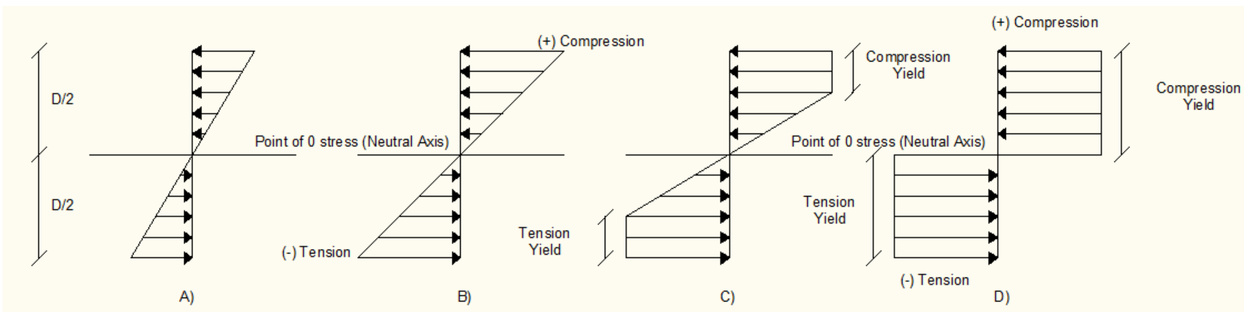

Figure 2.3: The progression of stresses as the load is applied to an isotropic and homogenous beam. A) Beam resisting service loads. B) Beam resisting loads that are on the edge of the yield stress of the material. C) Extreme fibers of the beam have begun to yield. D) All fibers in the beam are yielding (Bažant and Jirásek 2002).

The figure is for a material such as steel that is both isotropic and homogenous, thus the moduli of elasticity in tension and compression are equal. This is an idealized diagram and not realistic for wood. Since wood is an anisotropic and non-homogenous material, the neutral axis will shift up or down depending on the individual characteristics such as knots and grain angle, of the beam. The actual stresses in a wood beam would more closely resemble those depicted in Figure 2.4.

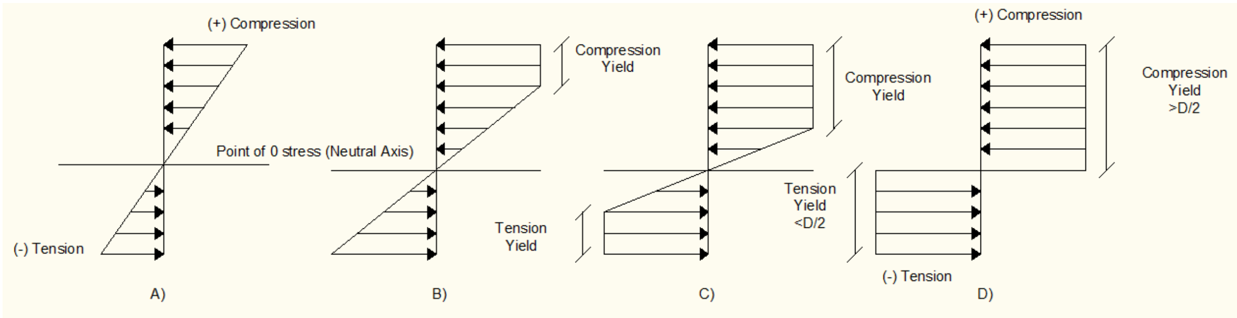

Figure 2.4: Rectangular cross section of a beam in pure bending. A) Beam resisting service loads. B) Beam resisting loads that exceed the compressive yield strength, the compression fibers begin to yield. C) Extreme tension fibers have began to yield. D) All fibers in the beam are yielding.

This figure shows that the modulus of elasticity for compression is less than that for tension, and thus the neutral axis is below the center of the beam. As the compression fibers begin to yield, the neutral axis moves downward, making the compression zone larger, and in turn the tension zone gets smaller. This type of behavior is what we expect to see in a clear wood beam. A knot is a discontinuity in the natural grain of the beam and is expected to cause the neutral axis to move away from the knot. This is expected because the internal forces in the beam need to equal zero, thus meaning that more fibers will have to be put in the zone that the knot is in to compensate for the separation of fibers.

2.3 Isotropic vs. Anisotropic Materials

An isotropic material is defined as a material which exhibits the same properties in all directions. A common example of an isotropic material is structural steel. Structural steel has the same modulus of elasticity in tension and in compression. On the other hand, a material such as wood is considered to be an anisotropic material. Being anisotropic, wood will exhibit different properties in different directions. The three principle directions are presented in relation to grain orientation in a wood beam in Figure 2.5.

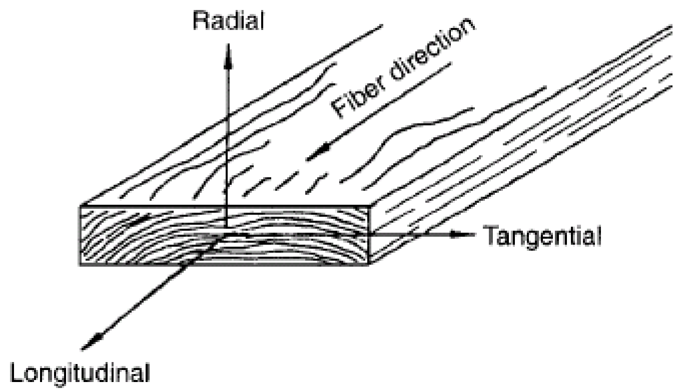

Figure 2.5: Shows the three principle directions in a wood beam with respect to wood grain orientation (Forest Products Laboratory 1999).

A growth ring can be defined as the natural growth of the tree that occurs each year as the tree goes through the grow season and then in to the dormant season. Trees that grow in warm, moist climates tend to have wider growth rings than trees grown in an arid climate that gets colder in the winter time. A force applied in the radial direction attempts to separate the growth rings in the wood grain. A force applied in the tangential direction will split the growth rings, while a force in the longitudinal direction attempts to stretch the fibers in the wood itself. It is apparent that the resistance to these forces will be different in all three of these directions thus making wood anisotropic. The ultimate strength of a wood beam will be at a maximum when it is subjected to forces perpendicular to the grain of the wood because it results in stresses which are parallel to the grain, where wood strength is the greatest.

2.4 Homogenous vs. Non-homogenous material

A homogenous material is a material that exhibits the same properties throughout. A non-homogenous material is the opposite of this, and its properties are different at different locations. For example, we can again compare steel and wood. Steel is considered homogenous because it is consistent throughout at macroscopic scales. Wood on the other hand is a non-homogenous material due to variations of the natural growth of a tree. These variations can be caused by a range of things including grain angle, width of growth rings, and of course, knots. These characteristics make wood a much more difficult material to analyze than an isotropic, homogenous material such as steel.

2.5 Behavior of Wood

Clear, straight- grained wood has been used in the past to determine the strength properties of wood that is used in design calculations. However it is obvious that wood in structural applications contains several natural defects like grain angle, pitch pockets, and knots. These defects must be taken into account when considering the realistic strength characteristics of a typical wood beam. The substance of which wood is composed has a specific gravity of about 1.5, meaning that it is denser than water. However, once the specimen is dried and in the state that it would be in when used as a building material, most species of wood float. This is confirmation that part of the wood structure is made up of pores or holes (Green et al. 1999). The ultimate strength will not be compromised by these pores but instead will be effected by the variation of grain angle and presence of knots.

When considering the strength of a beam, it has been seen that clear wood is much stronger in tension than it is in compression. In fact, according to the Forest Products Laboratory (1999), clear wood is nearly twice as strong in tension as it is in compression. This behavior is depicted in Figure 2.6 in the stress-strain curves of wood in tension and in compression. The stress- strain curves for both tension and compression start out being linear with equal slopes, however this changes part way up the curve as the compression curve starts to flatten out and moves much more quickly towards the failure point.

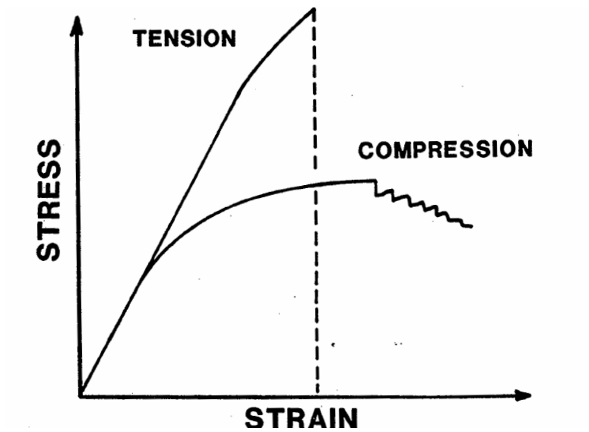

Figure 2.6: Schematic of Stress-Strain Curves of small, clear Wood in tension and in compression (Schniewind 1982)

2.5.1 Knots

A knot is a portion of a tree branch that has been incorporated into the main trunk of a tree. Knots tend to have a very large effect on the mechanical properties of wood, but the magnitude of the effect strongly depends on the size, shape, location, and local characteristics of the knot. The effect on mechanical properties occurs because a knot is an interruption of continuity and a change in the direction of wood fibers associated with the knot (Green et al. 1999).

There are several different classifications of knots. The first classification is the shape of the knot. The shape of any given knot in a wood beam depends highly on the direction in which the beam was sawn out of the tree. A circular knot is produced when a log is sawn through at right angles as compared to the growth direction of the branch. Most branches are nearly round, so sawing it at a right angle would produce a very nearly circular knot. The other type of knot is called an oval knot and occurs when the lumber is sawn from the log at some other angle that is not a right angle to the branch; this causes an elliptical or oval knot. The other classification that is applied to knots is whether the knot is intergrown or encased. An intergrown knot is often referred to as a tight knot and develops when a limb remains alive and there is continuous growth at the junction of the limb and the trunk of the tree. This continuous growth causes the grain to become intertwined with the branch in the trunk. An encased knot, often referred to as a loose knot, occurs when the branch dies and the additional growth of the trunk encases the knot. The tree fibers are not continuous with the fibers of the encased knot and this results in the knot becoming its own section in the tree. Encased knots also often result in knotholes. An encased knot and an intergrown knot are shown in Figure 2.7.

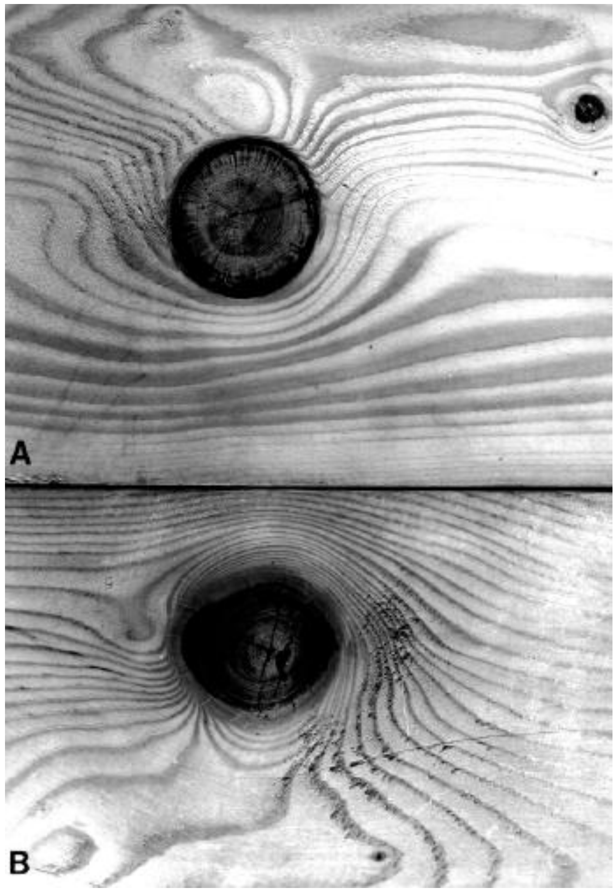

Figure 2.7: (A) encased knot, (B) intergrown knot (Green et al. 1999).

2.5.2 Slope of Grain

The term slope of grain relates the fiber direction to the cut edges of a beam. The slope of grain can be affected by the natural growth of the tree but it can also be affected by the way it was sawn in the mill. A slope in the grain can cause a severe loss of strength. The bending strength in a wood beam is at a maximum when the wood grain is perpendicular to the applied load. The wood grain being perpendicular to the applied load causes the internal stresses in the beam to be parallel to the grain (in the longitudinal direction). It can also be said that the strength of the beam is at a minimum when the wood grain is parallel to the applied load; a parallel grain causes the stresses to be perpendicular (in the radial or tangential direction) to grain. Table 2.1 shows a summary of the strength of wood members with various grain slopes compared with the strength of a straight-grained member.

Maximum slope of grain in member	Modulus of rupture (%)	Impact bending (%)	Compression parallel to grain (%)
Straight-grained	100	100	100
1 in 25	96	95	100
1 in 20	93	90	100
1 in 15	89	81	100
1 in 10	81	62	99
1 in 5	55	36	93

Table 2.1: Strength of wood members with various grain slopes compared with straight-grained members (Greenet al. 1999).

This table shows that the grain angle contributes a great deal to the overall strength of a wood beam in bending. Slope of grain is usually expressed by the ratio of 25 mm of the grain from the edge or long axis of the piece and the distance in millimeters within which this deviation occurs (Greenet al. 1999).

2.6 Related Works

In a thesis by Holm (2007), four 1 in x 1 in Douglas Fir beams were tested, each with different knot characteristics. The first beam was a clear specimen and of the other three beams, one had a knot in tension, one a knot in compression, and one had a knot in the center of the beam. In this test, the beams were subjected to the four-point loading as shown in Figure 2.8.

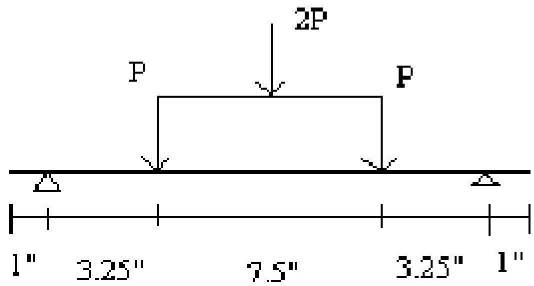

Figure 2.8: Test setup (Holm 2007)

The strain data were gathered using VIC-3D software and Digital Image Correlation equipment. In the clear beam, the average height of the neutral axis was 0.462 in above the bottom of the beam. This result was expected because the modulus of elasticity in tension is greater than the modulus of elasticity in compression, which means that the compression zone will be larger than the tension zone in order to produce an internal equilibrium of forces. As expected for the samples with knots in compression and in tension, the neutral axis moved away from the knot. A knot is a discontinuity in the grain which means that the beam will respond to this by having more fibers in compression, if the knot is in compression, or tension, if the knot is in tension. The modulus of elasticity for tension will decrease with a knot in tension, just as a knot in compression will cause a decrease in the modulus of elasticity for compression. The results of the testing by Holm are summarized in Table 2.2.

	Location of NA From Bottom of AOI (in)*			
Beam	**Left Edge**	**Mid-Section**	**Right Edge**	**Average**
Clear	0.474	0.457	0.457	0.462
Center Knot	0.500	0.612	0.457	0.564
Compression Knot	0.205	0.231	0.239	0.222
Tension Knot	0.655	0.733	0.733	0.715

*AOI = Area of Interest

Table 2.2: Summary of Results by Holm (2007).

The research done by Holm was followed up by Davis (2010). Davis expanded the research by not only testing 1 in x 1 in Douglas fir beams, but also testing clear 1 in x 1 in specimens of different species of wood including Southern Yellow Pine, Hem Fir, Alder, Oak, and an unknown species. The species of wood seemed to affect the position of the neutral axis slightly. The results show a slight variation of the location of the neutral axis among the various species, but all are consistently located below the centroid of the beam (Davis, 2010). The results started at a minimum of 0.40 inches from the bottom of the beam in the Hem Fir sample all the way up to a maximum value of 0.46 inches from the bottom of the beam in the Douglas Fir sample and the Southern Yellow Pine sample. The results of the testing done by Davis are summarized in Table 2.3.

Sample #	Specimen (clear)	Location of neutral axis relative to the tension face of the beam (in.)
1	Douglas Fir	0.46
4	Southern Yellow Pine	0.46
5	Hem Fir	0.40
6	Alder	0.44
7	Oak	0.45
8	Unknown Species	0.44

Table 2.3: Summary of the testing of different species of clear samples (Davis, 2010)

The testing done by Davis (2010) for multiple clear beams of different species was the same for the testing done by Holm (2007) in the Douglas Fir beam but different for the different species.

Davis showed that the neutral axis for Douglas Fir was higher than the neutral axis for wood beams of other species (it was the same for Southern Yellow Pine). This result shows that the modulus of elasticity for tension for species of Hem Fir, Alder, and Oak was much greater than the modulus of elasticity of compression for the same species. In the Douglas Fir sample, the fact that the neutral axis was nearer the center tells us that the modulus of elasticity in compression and in tension were closer than they were in the other species.

In addition to the 1 in x 1 in beams that were tested, Davis also tested a group of 2 in x 4 in Douglas Fir beams. Of these beams, one was a clear specimen, one contained a compression knot, one contained a tension knot, and one contained a knot in the center. These beams were not tested to failure and in each case, the beam was tested in one direction and then inverted to put the tension knot in compression and the compression knot in tension and tested again. It was found in the clear beam that the neutral axis was located at approximately 52% of the depth of the beam measured from the tension face. This is interesting because the neutral axis was located below the center of the beam in the 1 in x 1 in beams tested in the same way. This shows that the modulus of elasticity for compression in the 2 x 4 beam was greater than the modulus of elasticity for tension. This result is different than is assumed and was shown by Holm (2007) and Davis (2010) for 1in x 1in beams A summary of the results of the 2 in x 4 in beam tested by Davis (2010) can be found in Table 2.4.

Specimen	Total Length (in)	Depth of Beam (in)	Neutral Axis Location Relative to Tension Face of the Beam (in)
1a (clear)	63.75	3.52	1.82
1b (inverted, clear)	63.75	3.52	1.855
2a (compression knot)	69.5	3.51	1.575
2b (inverted, tension knot)	69.5	3.51	1.995
3a (center knot)	65.5	3.51	1.645
3b (inverted, center knot)	65.5	3.51	1.4
4a (tension knot)	54.5	3.49	2.065

Table 2.4: Summary of Results from 2 in x 4 in beams (Davis, 2010)

3.0 Experiment

Testing was done on ten nominal 2 x 4 wood beams, all containing knots in different locations along the beam. Specimens were chosen not at random, but picked in pairs to see the repeatability of the results. The first specimen was chosen as a control specimen with a relatively straight grain angle and contained no knots. The second specimen was chosen because of its interesting distribution of several knots directly in the center of the area of interest. There were then four different pairs of beams chosen because of their similar characteristics. The different pairs were organized as specimens 3 and 4, specimens 5 and 6, specimens 7 and 8, and specimens 9 and 10. One of these pairs was chosen with a random array of small knots and others contained a similar distribution of knots in the area of interest. Photos of the chosen specimens are shown below in Figures 3.1-3.10; larger photos can be found in Appendix B.

Figure 3.1: Specimen #1, Clear Specimen

Figure 3.2: Specimen #2

Figure 3.3: Specimen #3

Figure 3.4: Specimen #4

Figure 3.5: Specimen #5

Figure 3.6: Specimen #6

Figure 3.7: Specimen #7

Figure 3.8: Specimen #8

Figure 3.9: Specimen #9

Figure 3.10: Specimen #10

Before testing was performed, characteristics of each beam such as grain angle, grain inclination, percent sapwood, and percent hardwood were observed and recorded. These characteristics were taken by visual inspection in the length of the beam between the supports. These characteristics are recorded in Table 3.1.

Sample #	%Heartwood	%Sapwood	Grain Angle (Degrees)	Grain Inclination (Degrees)
1	0	100	20	0
2	0	100	30	5
3	0	100	45	3
4	40	60	50	5
5	10	90	20	0
6	0	100	0	0
7	15	85	15	5
8	10	90	45	7
9	0	100	15	3
10	0	100	10	0

Table 3.1: Summary of Beam Characteristics for each Specimen being Tested.

All specimens were chosen several weeks before testing was done and were stored in a climate-controlled room to obtain consistent moisture content (MC) across the selection. Before the beams were tested moisture content was was measured and the average MC for all ten specimens was 12.4%.

3.1 Specific Methods

Data were collected using the Digital Image Correlation (DIC) equipment and an analysis was done using the VIC-3D software (Correlated Solutions, 2005). In order for the software to analyze the strain in the specimens, it needs reference points. Reference points are generated by putting a speckle pattern on the specimen itself. The speckle pattern is produced by first painting the beam with a white base, then using black spray paint to carefully place a pattern of black speckles which are the correct diameter and correct density to collect accurate data. This correct diameter and density of the speckles is unique to each test setup and depends on factors such as distance from the camera, camera angle, and lighting. This is a trial and error process that can sometimes take several attempts to get correct. An example of the speckle pattern that was used in this experiment is shown in Figure 3.11.

Figure 3.11: Speckle pattern used for all specimens.

Using the speckle pattern, the software is able to track the movement of the speckles between images at different stages of loading and uses that data to produce strain plots and numerical strain data for analysis. In the software, an Area Of Interest (AOI) is selected manually by the user. The only data points analyzed are the ones contained within the certain specified AOI. The AOI was the full width of the beam (89 mm) and the length of the beam between the loading points (457 mm). This AOI is selected using a rectangular section as shown in Figure 3.12.

Figure 3.12: Area of Interest (AOI).

The software records several images during the loading procedure. In this particular test, five images were collected manually at four different stages of loading. Base images were recorded under no load and data images were recorded at 3000 N, 6000 N, and 9000 N. However, the VIC-3D software does allow for the user to set it up to record as many images per second as desired, automatically. The loading was set up as four point loading as pictured in Figure 3.12.

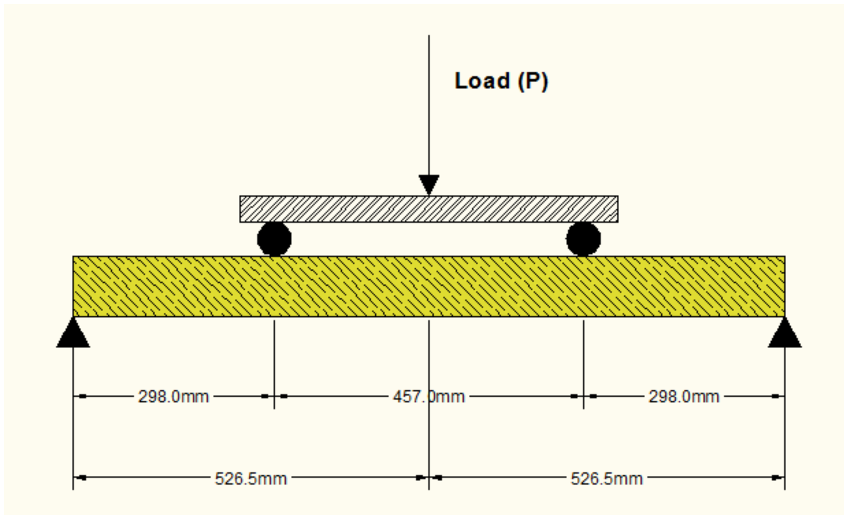

Figure 3.13: Test Setup Dimensions.

The camera setup is a very important part of the testing to ensure quality results. Two cameras with high resolution lenses are set up at an angle between 30 and 60 degrees of each other for optimum quality of results. It is very important that the cameras be aimed as close as possible to the same angle in reference to the beam so that geometrically, the points will move the same amount for corresponding images from both cameras. Consistent lighting of the specimen and the surrounding area is also crucial to obtain quality results. In this setup, an auxiliary lamp was used to achieve consistent lighting across the specimen. A diffuser was used to hang in front of the auxiliary light in order to lower the intensity of the lamp and get a more even distribution of light. The cameras are mounted on a tripod which holds them in the same position for testing every specimen. It is crucial that the cameras are not moved or refocused between specimens or during loading. The setup is very time intensive and is a trial and error process to determine the optimum lighting, angle, distance away from the specimen, etc. which will produce the best results. The cameras were set approximately three feet from the specimens. They were connected via wire to the computer that has the VIC-3D software. A photo of the overall test setup can be seen in Figure 3.14.

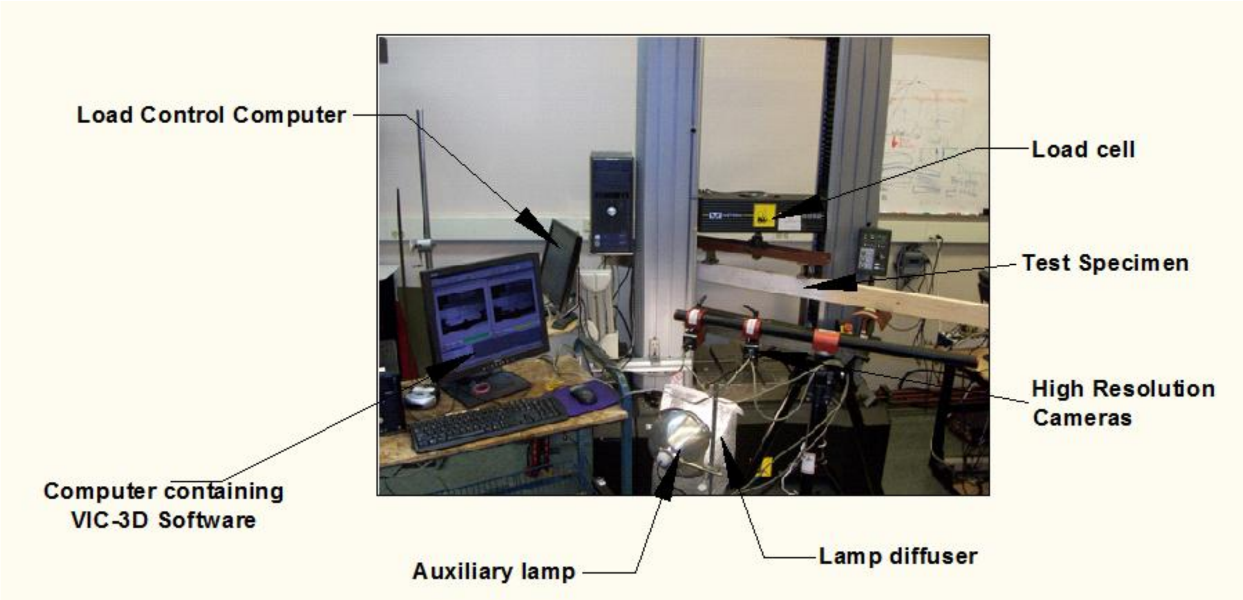

Figure 3.14: Test setup with the first specimen.

The cameras were mounted upside down to achieve a more direct camera angle. The computer with the VIC-3D software is in the left of the photo and the loading control computer is on the left and behind the computer with the VIC-3D software. The diffuser is pictured in the middle, bottom of the photo, and the load cell containing the specimen is in the middle of the photo near the wall. A perfect setup could not be achieved in this case due to size restrictions of the load cell. The load cell was not wide enough to provide a direct view of the specimen from the cameras. The specimen was forced to be placed in the load cell at an angle as can be seen in

Figure 3.14 and the cameras were set as close to perpendicular from the center of the area of interest as was possible given these restrictions.

3.2 Camera Calibration

Once the testing equipment is set up for testing, the cameras and the VIC-3D software must be calibrated to ensure that the correct focus, lighting, speckle pattern, etc. have been achieved for this specific test setup. Calibration is done by recording images of a calibration plate at varying locations around the image area, near the specimen. This calibration plate can be seen in Figure 3.15.

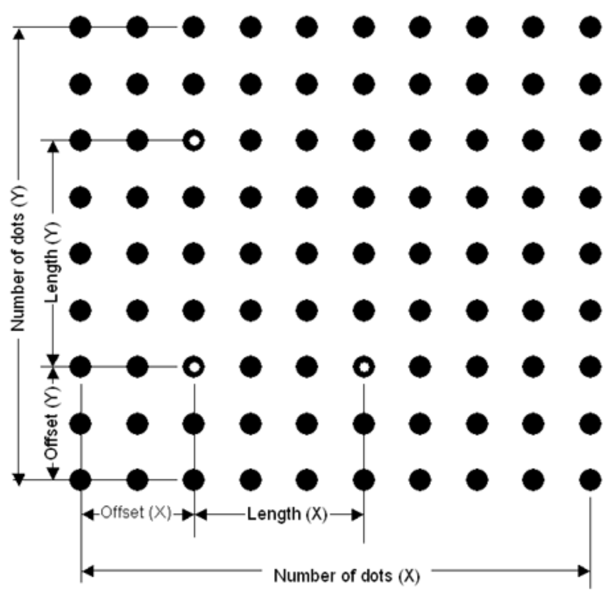

Figure 3.15: Calibration Plate (Holm, 2007)

A series of 35 images were taken from each camera at varying locations in the image area. The first set was taken with a straight-on orientation, the second set was taken at the same locations with the top of the plate tipped slightly toward the cameras, and the final set was taken at the same locations with the top of the plate tipped slightly away from the camera. The three open dots that are seen in Figure 3.15 must be recognized by the software in all images recorded during the calibration process. These images are analyzed by the software and a standard deviation of the results is produced. It is very important for the precision of the results that this standard deviation be less than 0.1. If a standard deviation of <0.1 is not achieved then the lighting, camera angle, speckle pattern or all of the above must be changed until the desired result is accomplished.

Once the desired standard deviation of the calibration images is achieved, the testing is now ready to begin. In this test, five reference images were taken at 0 N; these images are known as the reference images. The beam was manually loaded to 3000 N and five images were recorded at that point. This process was repeated for loads of 6000 N and 9000 N. These fifteen images are known as the deformation images. Three of the ten specimens failed before a load of 9000 N was applied. This was noted and reported in the results section. After the loading of the beam is finished and the images have been taken, the reference images and the deformation images are selected for analysis. Given that the setup and calibration of the cameras was successful, the VIC-3D software can track several coordinate points throughout the AOI on the beam.

3.3 Analysis

After the deformed images and reference images have been selected, the VIC-3D software can calculate the principal, shear, horizontal, and vertical strains from the partial derivatives of the displacement using the LaGrange strain tensor equations (VIC-3D manual). With these calculations, the program produces both a visual strain plot, as shown in Figure 3.16, and a numerical set of strain data, which was used to produce a graph of the location of the neutral axis with respect to X and Y coordinates.

Figure 3.16: Strain plot produced by the VIC-3D software.

The points that are shown on the strain plot in Figure 3.17 are also recorded manually in a .csv file that can be analyzed in Microsoft Excel. In Excel, the data are condensed down by disregarding all but the strain in the X direction (e_{xx}). A function which is able to sort out the X and Y coordinates was written and the data were then manually separated to exclude any irrelevant points. The points were then plotted as shown in Figure 3.17.

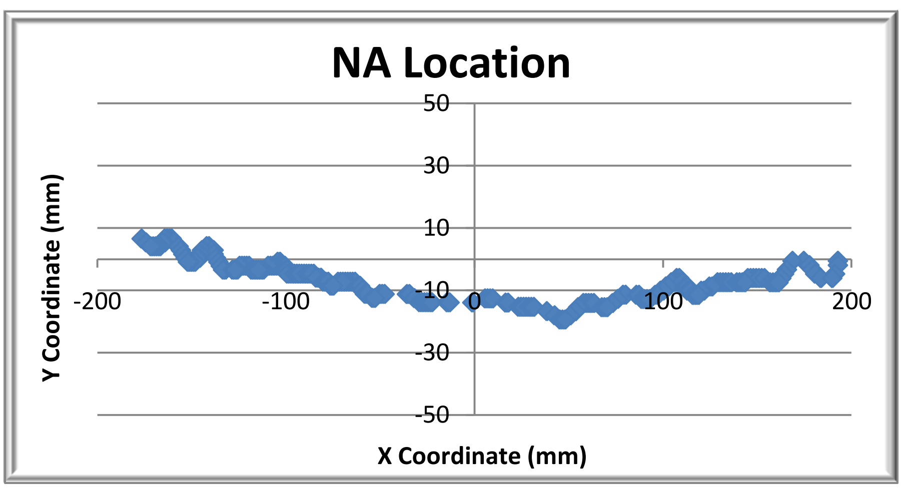

Figure 3.17: Plot of the location of the Neutral Axis.

Comparing the two plots, the one given by the VIC-3D software in Figure 3.16 and the one generated in Microsoft Excel using the VIC-3D numerical points, one can see that they follow each other nearly exactly.

3.4 Expected Results

From the literature and the results of two similar theses done by Oregon State University Honors College students, Sarah Holm and Phillip Davis, it is predicted that the neutral axis will move away from the knot whether it be in tension or in compression. Knots located in the center of the beam are expected to cause the neutral axis to move up or down depending on the differences in the modulus of elasticity in tension and compression for that particular beam as well as differences in characteristics such as grain angle in each of the beams and the looseness or tightness of the center knot. It is expected that the clear beam (specimen #1) will have a neutral axis slightly above the center of the beam as well as the two beams containing several small knots (specimens #5 and #6). It is not expected that the small knots will exhibit a large effect on the location of the neutral axis even in the local region. Specimen two containing a tight conglomeration of knots near the center of the area of interest will be interesting to observe. The effects of the knots are expected to nearly offset each other and the neutral axis will remain near the center of the beam. Pairs of specimens (#3 and #4, #5 and #6, #7 and #8, #9 and #10) containing similar patterns of knots will likely produce similar results.

4.0 Results and Discussion

The data were analyzed in strain plots produced by VIC-3D and graphs that were produced with numerical data in Microsoft Excel. Strain plots for each loading stage for each specimen can be found in Appendix C. The Microsoft Excel-produced graphs of the neutral axis can be found in Appendix D. A visual comparison was made for each of these plots to ensure that the data were consistent with the strain images. The plots were compared against the strain plot of the specimen in order to ensure that the numerical data was consistent with the visual strain data. It was also observed that the neutral axis moved away from the knots in the local region in most specimens just as expected. However, the pattern of the knots caused the effects of the knots on the location of the neutral axis to offset each other in some specimens which caused very little movement of the neutral axis.

4.1 Results

In each specimen, the visual strain images were exactly the same as the plotted version of the numerical data produced in Microsoft Excel. For clarity purposes, the numerical data were summarized in Table 4.11 which shows a minimum value, maximum value and average location of the neutral axis. The center of the beam was located using the coordinates of the AOI and all of the distances were in reference to the extreme tension fiber of the beam. The overall height of the 2 x 4 beams is 89 mm, so a value greater than 44.5 mm indicates that the neutral axis is above the center of the beam while a value less than 44.5 mm indicates the neutral axis is below the center. Figure 4.1 is an example of a strain plot and an Excel-produced neutral axis graph for the same wood specimen. The actual results will show the neutral axis as a region which gets smaller as the load increases, but for clarity purposes, the colors for the strain were narrowed to show the neutral axis as a line in the beam.

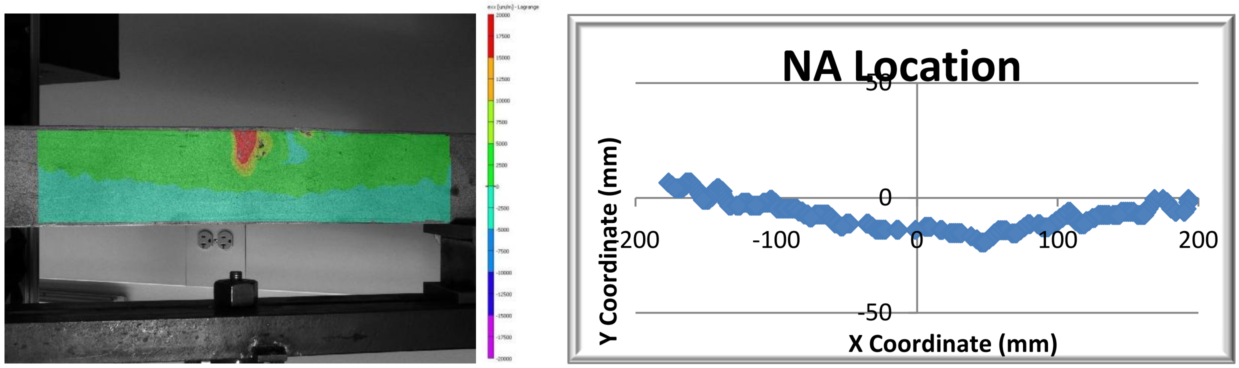

Figure 4.1: Strain plot and neutral axis graph of specimen 10 at a load of 9000 Newtons.

4.1.1 Clear Beam

The results for the location of the neutral axis in the clear beam were very nearly what was expected, and what was found in previous testing (Davis, 2010). The location of the neutral axis in reference to the bottom of the beam was a maximum of 52.25 mm and a minimum of 35.61 mm. The average location of the neutral axis in the clear beam was 45.12 mm above the bottom of the beam. This result was less than 1 mm above the center line, only slightly different from the results of Davis (2010). Davis showed that the average height of the neutral axis was 1.78 mm above the center line. The difference in results can be contributed to slight variations of the grain angle or other subtle characteristics in the clear beam that I selected and the clear beam selected by Davis. The numerical results are tabulated in Table 4.1. One can see that as the load increases, the average location of the neutral axis varies, but only slightly. The average values of the location of the neutral axis are all greater than 44.45 mm.

Load N	Maximum (mm)	Minimum (mm)	Average (mm)
3000	66.43	21.69	45.29
6000	56.33	37.45	45.68
9000	52.25	35.61	**45.12**

Table 4.1: Location of the neutral axis for the clear beam.

The reason that it is not exactly in the center comes back to what was discussed in the literature review section that wood is an anisotropic and non- homogenous material. Small imperfections in the wood and differences in modulus of elasticity for tension and compression will cause movement in the neutral axis. The strain plot of the clear beam loaded at 9000 N shows that the neutral axis stays near the center of the beam.

4.1.2 Specimen #2

Specimen #2 contained a tight array of knots in the center of the area of interest. In this case, the neutral axis stayed near the center of the beam as it passed through the knots, and the effects of multiple knots cancelled each other. In Table 4.2, one can see that the location of the neutral axis at a load of 7000 N moves down drastically from the previous load stages. It was noted in the experiment that this specimen failed at 7000 N, which would explain the severe change in the neutral axis. When the beam failed, the wood fibers were disrupted to an extreme sudden change in the location of the neutral axis occurred. Data were taken at the 7000 N load stage, but it was assumed that the location of the neutral axis of this beam at full load occurred at 6000 N. By visually inspecting the beam, it is seen that the positioning of the knots and characteristics of the tension knots and the compression knots are nearly the same so it makes sense that the neutral axis would move minimally. At a loading of 6000 N, the minimum height of the neutral axis was 38.68 mm above the bottom of the beam and the maximum height was 51.28 mm above the bottom of the beam. The average location of the neutral axis was calculated to be 45.58 mm from the extreme tension fiber. The numerical results for testing of specimen #2 are summarized in Table 4.2.

Load (N)	Maximum **(mm)**	Minimum **(mm)**	Average **(mm)**
3000	60.52	30.88	45.13
6000	51.28	38.68	**45.58**
7000	45.19	29.18	52.10

Table 4.2: Summary of results for specimen #2

4.1.3 Specimens #3 and #4

Specimens #3 and #4 were chosen as a pair due to similarities in knot distribution. Specimen #3 contained a tight knot in compression, a loose knot in compression, and a tight knot in tension. Specimen #4 contained a tight knot in compression, a tight knot in tension, and a tight knot near the center of the beam. It was also interesting to note that the positions of the knots in specimen #3 were close to each other along the length of the beam. The result for specimen was not as expected in a beam with these types of knots. It was expected that the location of the neutral axis would move up or down when it was in the vicinity of at knot. It was found, however, that the knots did not have a large effect on the location of the neutral axis. Since of the knots were located in the tension and compression zones, the neutral axis stayed very near the center of the beam. In the case of specimen #3, the maximum height of the neutral axis was 48.06 mm above the bottom of the beam and the minimum height of the neutral axis was 35.44 mm above the bottom under a full load of 9000 N. The NA was observed to be higher on the beam on the left side and then it consistently dropped toward the bottom of the beam as it moved to the right side of the area of interest. The average height of the NA in this specimen was 43.59 mm above the extreme tension fiber. The numerical results of this test are tabulated in Table 4.3.

Load	Maximum	Minimum	Average
(N)	**(mm)**	**(mm)**	**(mm)**
3000	52.19	35.34	41.73
6000	49.39	35.33	42.22
9000	48.06	35.44	**43.59**

Table 4.3: Summary of results for specimen #3

Unlike specimen #3, the results of specimen #4 were much closer to what would have been expected of a beam containing this type of knot pattern. The neutral axis showed a response to each of the tension and compression knots as it moved away from them in the local area. The NA moves further in to the compression zone for the center knot and the knot in tension, and moves toward the tension zone for the knot in compression. The maximum value at the maximum load of 6000 N was 69.45 mm above the bottom of the beam and the minimum value was 31.39 mm above the bottom of the beam. The NA begins very near the center of the beam on the left side of the AOI, then moves up in to the compression zone as it approaches a knot in tension. It then moves downward as it passes by the knot in compression. Once past the tension knot, the NA seems to settle to a location just below the center of the beam as it passes the center knot and continues on to the right side of the AOI. Note that this beam was not fully loaded. Failure occurred at 7500 N. The numerical data for the location of the neutral axis in specimen #4 are summarized in Table 4.4.

Load	Maximum	Minimum	Average
(N)	**(mm)**	**(mm)**	**(mm)**
3000	69.45	26.98	42.81
6000	61.94	31.39	**47.82**

Table 4.4: Summary of results for specimen #4

It is assumed that the differences in results between the #3 and #4 specimens can be contributed to the knot distribution along the length of the beam. The knots in specimen #3 are closer together which makes them more likely to offset each other. The knots in specimen #4 are farther apart which indicates that the knots will act more independently of each other.

4.1.4 Specimens #5 and #6

Specimens #5 and #6 contained an array of sporadically placed small knots. These knots were tight knots, and it was expected that they would not affect the location of the neutral axis a great deal. It was expected that the results of these two beams would be very similar to the results of the clear beam. The results did indeed turn out as expected and the behavior of the neutral axis was very much like the clear beam in both specimen #5 and specimen #6. The maximum value above the bottom of the beam for specimen #5 was 53.05 mm and minimum value of 38.10 mm at a the highest loading stage of 9000 N. The average value of the distance away from the extreme tension fiber for the location of the neutral axis was 47.85 mm. This value is farther away from the center of the beam than the clear span specimen but the result could be contributed to other factors such as grain angle affecting the location of the neutral axis. The results for the location of the neutral axis for specimen #5 are summarized in Table 4.5.

Load (N)	Maximum **(mm)**	Minimum **(mm)**	Average **(mm)**
3000	72.96	28.40	48.18
6000	55.61	39.49	47.77
9000	53.05	38.10	**47.85**

Table 4.5: Summary of results for specimen #5

Specimen #6 responded very similarly to specimen #5, which was expected. The minimum height of the neutral axis was 37.57 mm from the bottom of the beam and the maximum height of the neutral axis was 52.52 mm from the bottom of the beam at a load of 9000 N. The average location of the neutral axis was calculated to be 46.73 mm above the extreme tension fiber. The results for specimen #6 are shown in Table 4.6.

Load	Maximum	Minimum	Average
(N)	**(mm)**	**(mm)**	**(mm)**
3000	61.67	33.55	48.27
6000	54.11	36.19	47.23
9000	52.52	37.57	**46.73**

Table 4.6: Summary of results for specimen #6

The neutral axis stayed very near the center throughout the length of the beam for both specimens in the pair. This indicates that small, tight knots have little effect on the location of the neutral axis. This result was expected.

4.1.5 Specimens #7 and #8

When this pair was chosen it was thought that specimens 7 and 8 may be the pair that closest resembles each other in knot distribution pattern. Both of the specimens contained a tight knot in compression, a loose knot in compression, and a tight knot in tension. The distribution pattern also seemed to be similar in both specimens. After the testing, however, the two beams responded completely differently to the loading. To start with, specimen #7 failed at a load of 5200 N, while specimen #8 resisted the last stage of loading which was 9000 N. Not only were the ultimate strengths of the two beams different, but the location of the neutral axis of each beam was different as well. The neutral axis for specimen #7 responded only slightly to the knots as it moved down around the knot in compression, up around the tension knot, and back down away from the second knot in compression. The maximum height of the NA in specimen #7 was 56.24 mm above the bottom of the beam and the minimum height was 27.71 mm from the bottom. The average location of the neutral axis was 46.31 mm from the extreme tension fiber. The results of the testing of specimen #7 can be seen in Table 4.7.

Load	Maximum	Minimum	Average
(N)	**(mm)**	**(mm)**	**(mm)**
3000	56.24	27.71	**46.31**

Table 4.7: Summary of the results for specimen #7

The neutral axis moved as expected in specimen #8; it moved toward the tension zone for the knots in compression and toward the compression zone for the knot in tension. The greatest movement can be observed on the strain plot for the loose knot in compression. In the area near the loose knot in compression, the NA moved distinctly toward the tension zone. This makes sense because there is a substantially larger amount of strain in the area surrounding the loose knot than there is in the area surrounding the tight knot or a location on the beam with no knots at all as shown in the strain image. The maximum height of the NA above the bottom of the beam is 55.77 mm and the minimum distance above the bottom of the beam is 29.25 mm. The average height of the NA throughout the length of the area of interest is 45.00 mm which is very near the center of the beam. This average does not reflect the overall local movement of the NA as it moves in the area around the different knots. The numerical data for specimen #8 are summarized in Table 4.8.

Load	Maximum	Minimum	Average
(N)	**(mm)**	**(mm)**	**(mm)**
3000	61.77	22.91	45.70
6000	66.35	27.99	45.69
9000	55.77	29.25	**45.00**

Table 4.8: Summary of the results for specimen #8

4.1.6 Specimens #9 and #10

The similarities between specimen #9 and specimen #10 are that both specimens contain a tight knot in tension and a tight knot in compression. The differences are that in specimen #9 the knots are located very close to each other over the length of the beam and the knots in specimen #10 are spaced out a great deal farther over the length of the beam. This distinct difference turns out to be very important when considering the knots' effect on the location of the neutral axis. It can be seen in specimen #9 that there is very little movement in one direction or the other of the location of the NA as it passes by the knots. This is because the knots are very similar and have similar affects on the NA. If there was only one knot in tension in this beam, the location of the neutral axis would move down in to the compression zone of the beam, and likewise, in to the tension zone if only the compression knot were present. As it is, the effects of the two knots seemingly offset each other, and the result is that the neutral axis remains at a very consistent height throughout the length of the AOI. The maximum value for the location of the NA above the bottom of the beam is 52.07 mm and the minimum value is 41.10 mm at the last stage of loading of 9000 N. The average value of the height of the neutral axis is 45.70 mm above the extreme tension fiber. The results for the location of the neutral axis in specimen #9 are summarized in Table 4.9.

Load (N)	Maximum **(mm)**	Minimum **(mm)**	Average **(mm)**
3000	67.59	27.96	45.29
6000	52.96	38.29	45.80
9000	52.07	41.10	**45.70**

Table 4.9: Summary of the results for specimen #9

Specimen #10 on the other hand responded quite differently from specimen #9. The neutral axis begins near the center of the beam on the left side of the area of interest and tends to move upward, into the compression zone as it nears the knot in compression. The strain diagram shows severe strain in the knot in tension which tells us that it may have been slightly looser than was originally observed. After it passes by the tension knot, the neutral axis begins to fall sharply into the tension side of the beam as it gets nearer to the compression knot. This behavior is what was expected. The difference in the reactions of the NA in specimens #9 and #10 can be accredited to the longitudinal location along the AOI. The knots in specimen #10 were spread farther apart meaning that the effects of the two knots did not offset each other and instead both caused the location of the neutral axis to move. The maximum distance above the extreme tension fiber was 63.88 mm and the minimum height was 37.84 mm at a loading stage of 9000 N. The average location of the neutral axis over the entire span of the AOI was 51.07 mm above the extreme tension fiber. The results for specimen #10 are summarized in Table 4.10.

Load (N)	Maximum **(mm)**	Minimum **(mm)**	Average **(mm)**
3000	69.32	22.73	50.22
6000	61.21	34.06	49.63
9000	63.88	37.84	**51.07**

Table 4.10: Summary of the results for specimen #10

4.2 Summary of Results

The location and movement of the neutral axis varied greatly between specimens and between the knots in those specimens. It was seen in some beams that the knots in tension and the knots in compression had very nearly equal effects on the neutral axis and, in fact, the result was very little movement in its local location. Since there were multiple knots in these specimens, perhaps it is more informational to observe the minimum and maximum values that the neutral axis experienced rather than the average location. The results of the testing are shown in Table 4.11.

	Load	Maximum Location	Minimum Location	*Average Location pf NA
	(N)	**(mm)**	**(mm)**	**NA (mm)**
	3000	66.43	21.69	45.29
Specimen #1	6000	56.33	37.45	45.68
	9000	52.25	35.61	**45.12**
	3000	60.52	30.88	45.13
Specimen #2	6000	51.28	38.68	**45.58**
	7000	45.19	29.18	52.10
	3000	52.20	35.34	41.73
Specimen #3	6000	49.39	35.33	42.22
	9000	48.06	35.44	**43.59**
	3000	69.45	26.98	42.81
Specimen #4	6000	61.94	31.39	**47.82**
	NA	**NA**	**NA**	**NA**
	3000	72.96	28.40	48.18
Specimen #5	6000	55.61	39.49	47.77
	9000	53.05	38.10	**47.85**
	3000	61.67	33.55	48.27
Specimen #6	6000	54.11	36.19	47.23
	9000	52.52	37.57	**46.73**
	3000	56.24	27.71	**46.31**
Specimen #7	**NA**	**NA**	**NA**	**NA**
	NA	**NA**	**NA**	**NA**
	3000	61.77	22.91	45.70
Specimen #8	6000	66.35	27.99	45.69
	9000	55.77	29.25	**45.00**
	3000	67.59	27.96	45.29
Specimen #9	6000	52.96	38.29	45.80
	9000	52.07	41.10	**45.70**
	3000	69.32	22.73	50.22
Specimen #10	6000	61.21	34.06	49.63
	9000	63.88	37.84	**51.07**
*Neutral Axis is measured				
above the extreme tension fiber				

Table 4.11: Summary of Results for the Location of the Neutral Axis

4.3 Development of the Neutral Axis

Strain data were taken at 3 different levels of loading, 3000 N, 6000 N, and 9000 N. This type of progression shows the strain plots and the neutral axis as the beam advances towards its ultimate strength. The strain images were taken with fewer colors for simplicity sake but how jagged the line is shows that coordinates for zero strain were taken in a region. This region gets smaller and smaller with the increase of the load, shown by the line being less jagged at higher load cases. We can see in Figure 4.2 that the neutral axis begins to straighten out and become less jagged as a higher load is applied.

Specimen #8 (Two tight knots in compression, tight knot in tension)

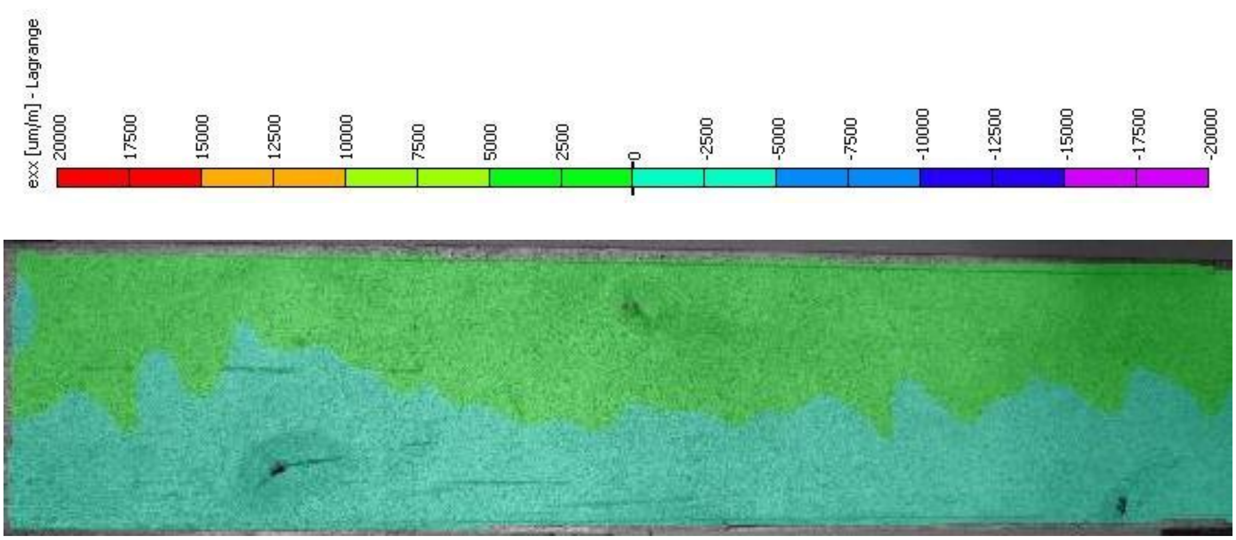

Load: 3000 N

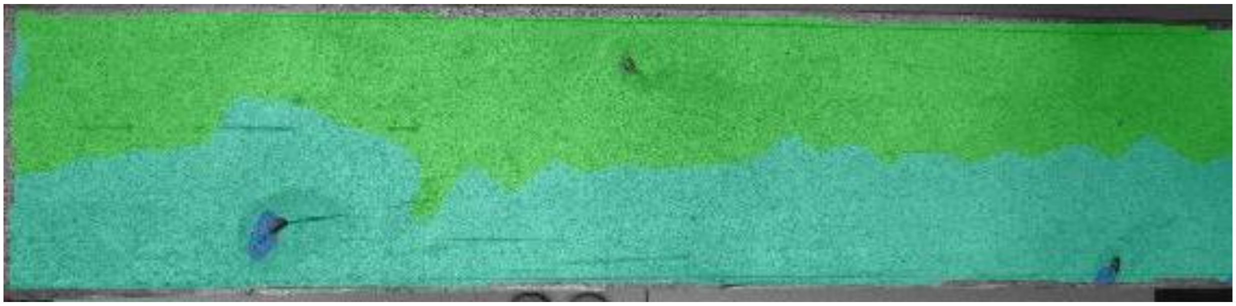

Load: 6000 N

Load: 9000 N

Figure 4.2: Development of the neutral axis.

4.4 Comparison of Theoretical to Observed Strains

In order to confirm that the results reported in this paper were practical and consistent with theory, a comparison of the theoretical strain and the observed strain was made. The equations and calculations of this comparison can be seen in detail in Appendix A. A modulus of elasticity was calculated for each of the specimens depending on the load applied to the beam and the resulting deflection. The results of this calculation yielded a maximum percent difference between the calculated strain and the observed strain of 51% and a minimum percent difference of 7%. These percent differences were very small thus confirming that the data taken in this testing was relevant to the theory used to analyze stresses and strains in wood beams. The strain calculation comparison was done at a load of 3000 N in order to assume a linear elastic behavior of the beams. The differences could also be attributed to the fact that the neutral axis is a band when at a low load such as 3000 N rather than a well- defined line. The band is represented in the strain images by the jagged line which is the neutral axis. This could cause assumption problems in the strain calculations as well.

5.0 Conclusions

When comparing these results to the work done by Holm (2007) and Davis (2010), there are many similarities in the results but there are several differences as well. Holm and Davis both explored wood beams containing just a single knot instead of a pattern of knots in different locations along the length of the area of interest. They found that as the load was applied to the beam, the neutral axis would move away from the knot. They also found that in the clear specimens of 1 in x 1 in beams, the average height of the neutral axis was slightly below the centroid of the beam. Davis found in his testing of the 2 x 4 beams that the neutral axis was 1.82 inches from the tension face of the beam which means that it is 54% away from the tension face. This was an interesting discovery because it was on the compression side of the center of the beam rather than the tension side as was found for the 1 in x 1 in beams. It was found in my testing that the average location of the neutral axis in the clear beam was 45.12 mm from the tension face of the beam. In a beam that is 89 mm wide, this makes the location of the neutral axis 50.7% of the way above the tension face. The results by Davis (2010) were slightly different. The average location of the neutral axis in the clear 2 x 4 beam tested by Davis was 1.1 mm higher than the average location of the neutral axis in my clear beam. This difference is contributed to subtle differences in grain angle and other characteristics in the two clear span beams.

The testing done by Holm (2007) and Davis (2010) showed a consistent movement in the average location of the neutral axis throughout the beam with beams with a single knot. The results found in this thesis did not find the same average location difference. This is because the beams containing multiple knots tended to average the location of the neutral axis near the center. The neutral axis would move away from a compression knot, then move away from a tension knot and magnitudes of the movement tended to offset each other, and show only a minor net average movement of the neutral axis over the span of the beam. In some cases, where the knots were longitudinally placed close together, the neutral axis showed little to no movement at all. This shows that the effects from the knots are effectively cancelling each other out and the neutral axis is not affected. It was found that the existence of multiple knots in a wood beam affects the location of the neutral axis locally around the knot as found by Holm (2007) and Davis (2010), but when equal numbers of knots are in tension and in compression, the overall average movement most often is very small.

6.0 Future Work

In order to obtain a better understanding of the local movement of the neutral axis in wood beams with knots, more testing needs to be done. Ideally, the testing would be with a wider range of specimens and contain knots with more extreme characteristics. It would be ideal to test a beam containing a large, loose knot in one of the zones, then a small tight knot in the other zone and see how that would affect the movement and overall average location of the neutral axis. The selection of beams with similar patterns of knots was to produce similar results within the pair. This, however, was not the case. As shown in many of the pairs, the characteristics of the knots, rather than the location of them seemed to make a larger difference. I believe that if testing was done considering the characteristics of the knots as well as the position of them along the beam and in the tension/compression zones, conclusions could be drawn on how different types of knots affect the movement of the average height of the neutral axis in wood beams containing multiple knots with similar characteristics. More research needs to be done in order to confirm any of the findings that are reported within this paper.

REFERENCES

- ASTM 2009 Standard test methods of static tests of lumber in structural sizes. Designation: D 198 - 08. Annual Book of ASTM Standards, Sec. 4 (Construction), Vol. 04.10. West Conshohocken, PA.

- Bažant, Z. and Jirásek, M. (2002). *Inelastic Analysis of Structures.* John Wiley & Sons, Ltd. West Sussex, England. pp. 351-353.

- Bedford, A., and K. Liechti. *Mechanics of Materials*. 1st. Upper Saddle River, NJ: Prentice Hall, 2000. 627 pp.

- Correlated Solutions. (2005). *Vic-3D User Manual.* Correlated Solutions, Inc. Columbia, SC.

- Davis, P. 2010. An Examination of the Neutral Axis of Wood Beams. University Honors College Thesis, Oregon State University. pp. 19-22.

- Forest Products Laboratory (1999). *Wood Handbook: Wood as an Engineering Material. General Technical Report.* U.S. Department of Agriculture, Forest Service, Forest Products Laboratory, Madison, WI. 463 pp.

- Gere, J. and Timoshenko, S. (1997). *Mechanics of Materials* (4th Edition). PWS Pub. Co., 912 pages.

- Green, D.W., Winandy, J.E., Kretschmann, D.E. (1999). *Mechanical Properties of Wood*. Wood handbook : wood as an engineering material. Madison, WI : USDA Forest Service, Forest Products Laboratory, 1999. General technical report FPL ; GTR-113: pp. 4.1-4.45.

- Holm, S. 2007. Location of the Neutral Axis of Wood Beams. University Honors College Thesis, Oregon State University. 70 pp.

- Kollman F. and Cote, W. (1968). *Principles of Wood Science and Technology I: Solid Wood.* Springerverlag, New York. 419 pp.

- Redler, H. “Movement of Neutral Axis in Beams Subjected to Pure Bending.” Submitted for a Reading and Conference Course class to Dr. Rakesh Gupta at Oregon State University. Corvallis, OR. 2006.

- Schniewind, A. *Mechanical Behavior and Properties of Wood.* University Park, PA: 1982. 56-94

Appendix A: Strain Calculations

In order to verify that the results are consistent with the theoretical values of strain calculated, a check must be performed on the results. The following five equations were used to check the strains in the specimen obtained during testing. These equations are relevant for the four point loading shown in the figure.

$E = \frac{Pa^2}{6\Delta I}(3L - 4a)$ $\quad I = \frac{bh^3}{12}$ $\quad M = \frac{P}{2} * a$

$\sigma = \frac{Mc}{I}$ $\quad \varepsilon = \frac{\sigma}{E}$

$E = modulus\ of\ elasticity$

$P = single\ applied\ load$

$a = distance\ from\ support\ to\ point\ load\ (298\ mm)$

$\Delta = deflection\ at\ midspan$

$I = moment\ of\ inertia$

$L = span\ length\ of\ beam$

$b = base\ length\ of\ beam$

$h = height\ of\ beam$

$M = moment\ at\ midspan$

$c = height\ of\ compression\ zone$

$\sigma = stress\ at\ midspan$

$\varepsilon = strain\ in\ beam$

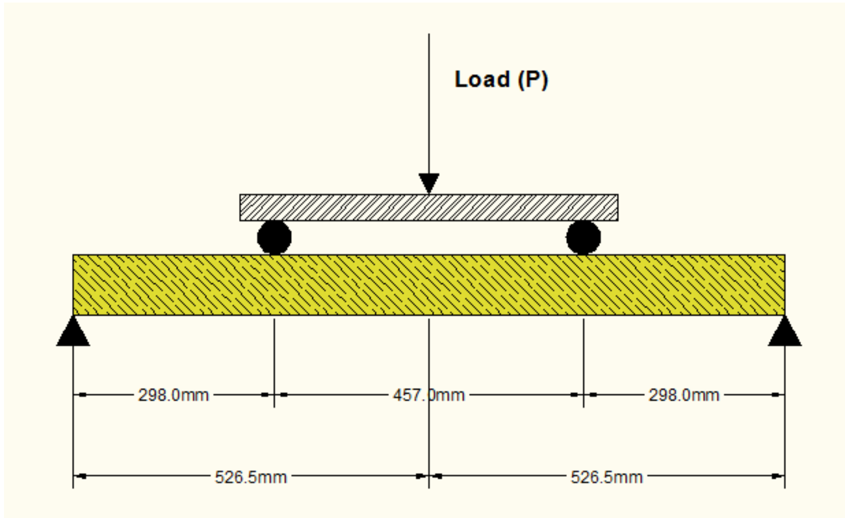

Four Point Loading

The calculations for the strain in the beams during testing are computed for the 3000 N load case. This strain will be compared to the observed strain in the data produced by VIC-3D.

The moment of inertia, *I*, will be the same for all of the 2 in x 4 in wood beams. The beams that were used were planed to a total dimension of 1.5 in x 3.5 in (38.1 mm x 88.9 mm), and the calculation of the moment of inertia for these beams is shown below.

$$I = \frac{bh^3}{12} = \frac{38.1*88.9^3}{12} = 2.23x10\text{^}6\ mm^4$$

The modulus of elasticity for each beam was calculated using the above equations. The length, L, was 1053 mm and the distance from either applied force to the support is 298 mm for every beam. The values for P and Δ were taken in the portion of the beam where the loading was linear as a point estimate. The calculated strain and the observed strain along with a percent difference are shown below. The observed strain and the calculated strain are very close to each other; the largest percent difference is 51% which could be contributed to assumptions in the strain calculation such as assuming that the internal stresses are linear. The closeness of the reported and the calculated strains means that the data that was collected was quality data and the results of the location of the neutral axis are relevant to reality.

Specimen	Deflection (mm)	E (Gpa)	Δ (mm)	P (N)	c (mm)	σ (Gpa)	ε (observed)	ε (calculated)	% Difference
1	2.255	17.36	2.255	3000	40.7	0.008156	0.000410	0.000470	15
2	3.669	10.67	3.669	3000	40.1	0.008035	0.000841	0.000753	10
3	3.551	11.03	3.551	3000	44.8	0.008977	0.000760	0.000814	7
4	3.197	12.25	3.197	3000	32.29	0.006470	0.000350	0.000528	51
5	2.993	13.08	2.993	3000	42.31	0.008478	0.000756	0.000648	14
6	3.145	12.45	3.145	3000	42.8	0.008576	0.000510	0.000689	35
7	3.559	11.00	3.559	3000	38.32	0.007679	0.000920	0.000698	24
8	3.071	12.75	3.071	3000	39.27	0.007869	0.000480	0.000617	29
9	3.025	12.94	3.025	3000	43.54	0.008725	0.000798	0.000674	16
10	3.239	12.09	3.239	3000	30.5	0.006112	0.000890	0.000506	43
					I=	2230740	**mm^4**		
					M=	447	**N-m**		

Appendix B
Test Specimen Photos

All beams were Douglas Fir, 2 x 4

Test Specimen #1 (Clear Beam)

Test Specimen #2 (Tight group of knots in the center of the beam)

Test Specimen #3 (Tight knot in compression, loose knot in compression, tight knot in tension)

Test Specimen #4 (Tight knot in compression, tight knot in tension, tight knot near the center)

Test Specimen #5 (Random array of small knots throughout AOI)

Test Specimen #6 (Random array of small knots throughout AOI)

Test Specimen #7 (Tight knot in compression, loose knot in compression, tight knot in tension)

Specimen #8 (Two tight knots in compression, tight knot in tension)

Specimen #9 (Tight knot in compression, tight knot in tension)

Specimen #10 (Tight knot in compression, tight knot in tension)

Appendix C
Strain Plots

***Note: Cameras were placed upside down so the presented top of the beam is in tension and the bottom in compression.**

Specimen #1 (Clear Beam)

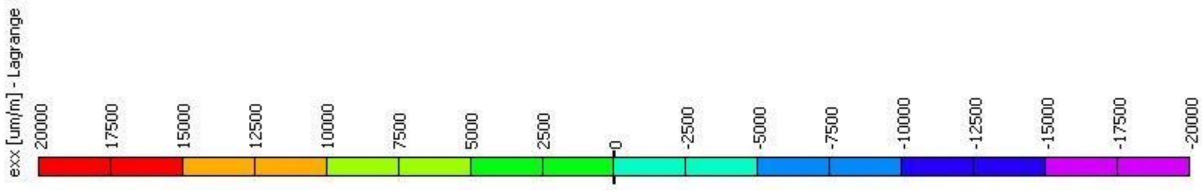

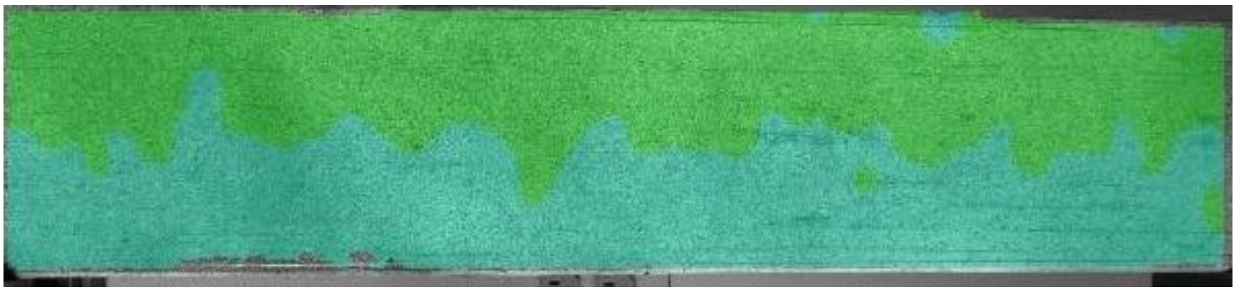

Load: 3000 N

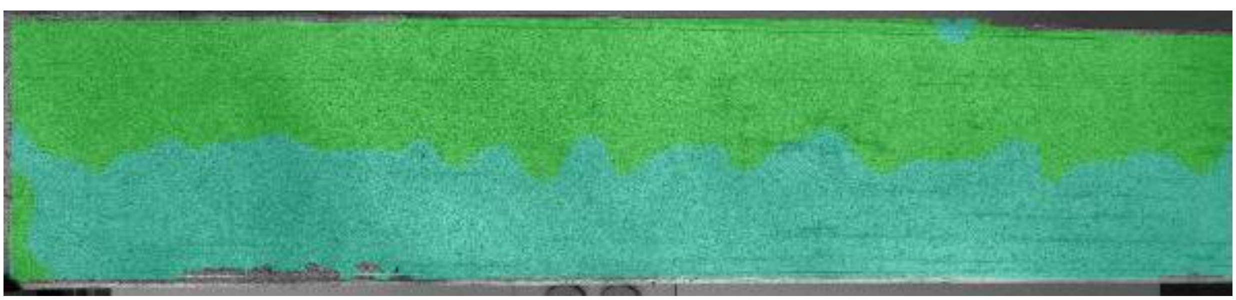

Load: 6000 N

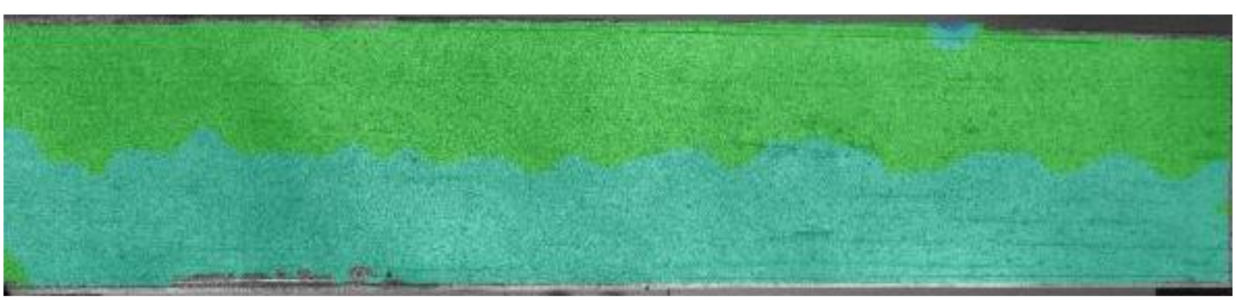

Load: 9000 N

Specimen #2 (Tight group of knots near the center of the beam)

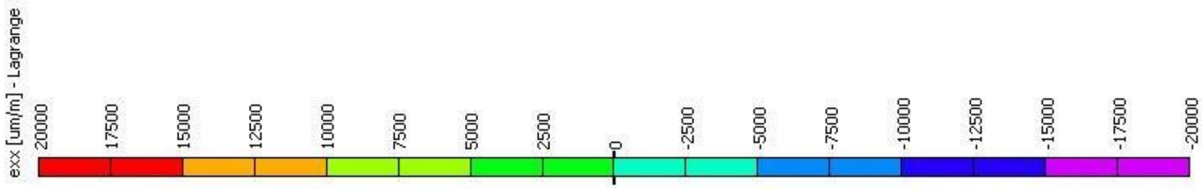

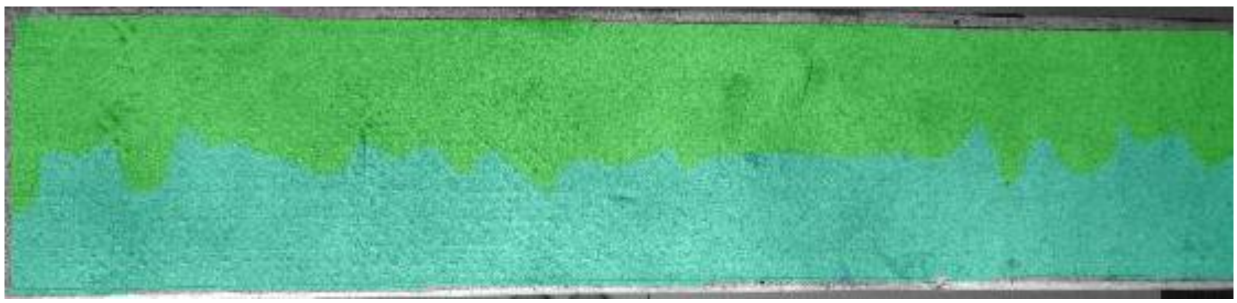

Load: 3000 N

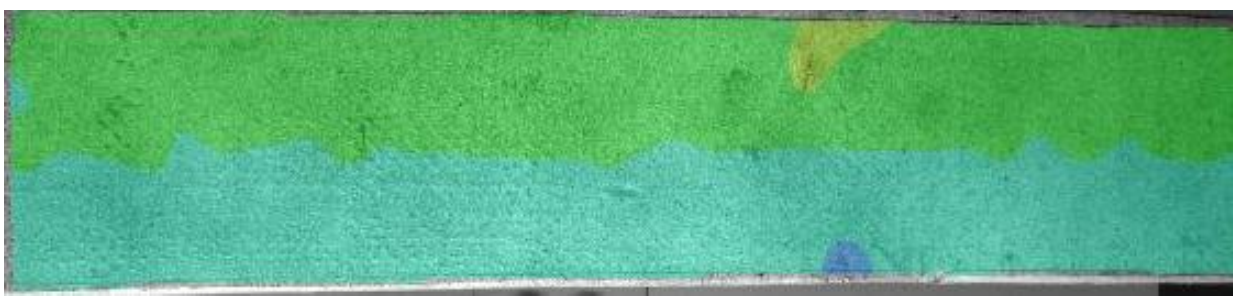

Load: 6000 N

Specimen #3 (Tight knot in compression, loose knot in compression, tight knot in tension)

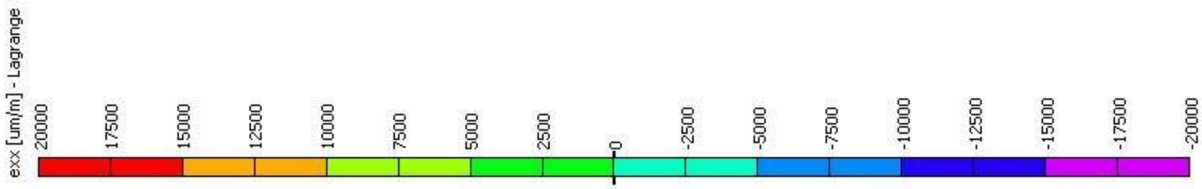

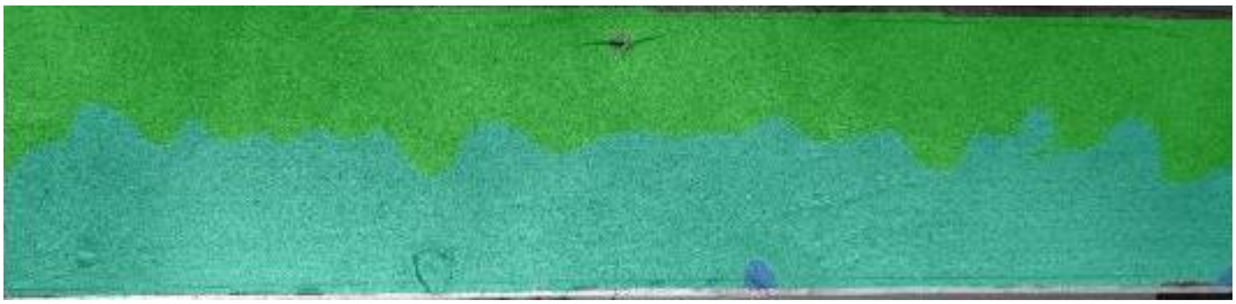

Load: 3000 N

Load: 6000 N

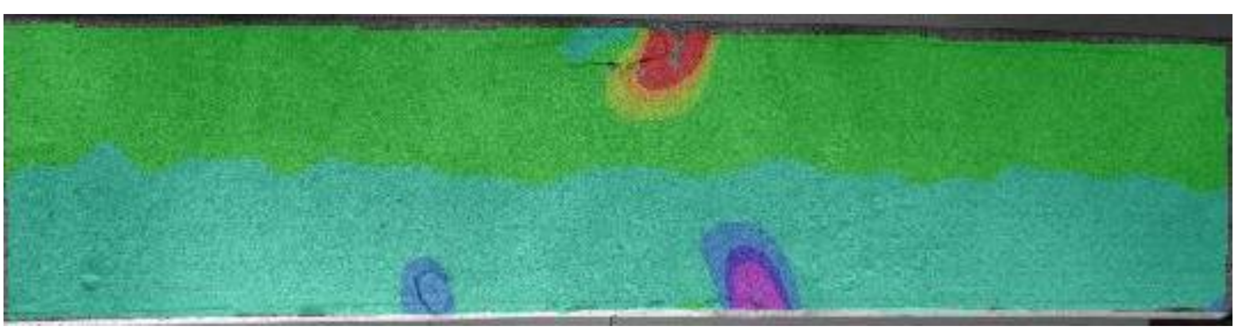

Load: 9000 N

Specimen #4 (Tight knot in compression, tight knot in tension, tight knot near the center)

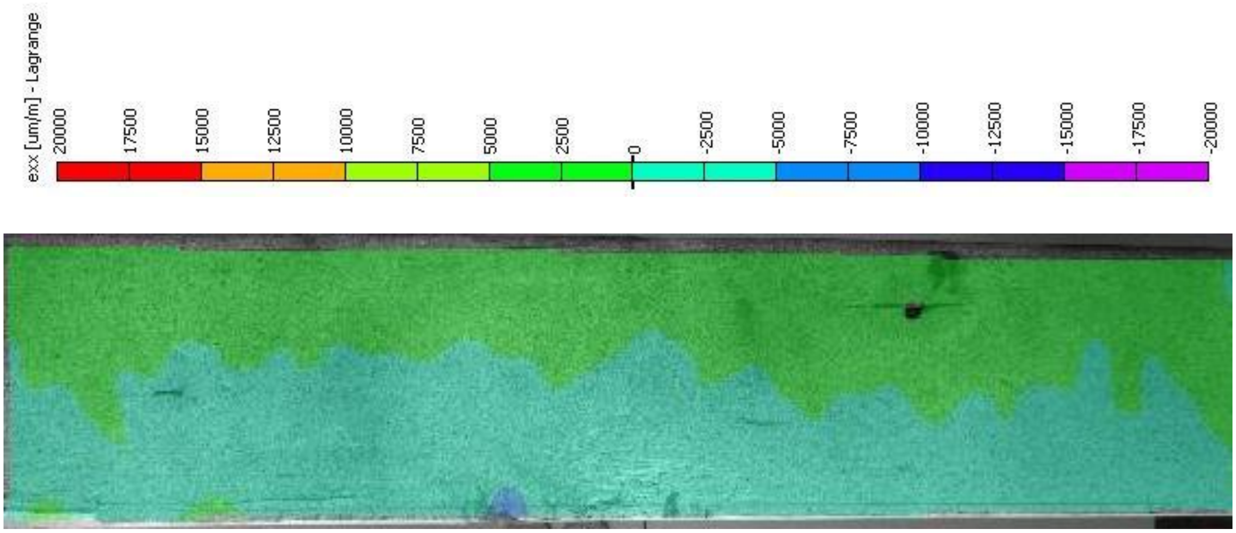

Load: 3000 N

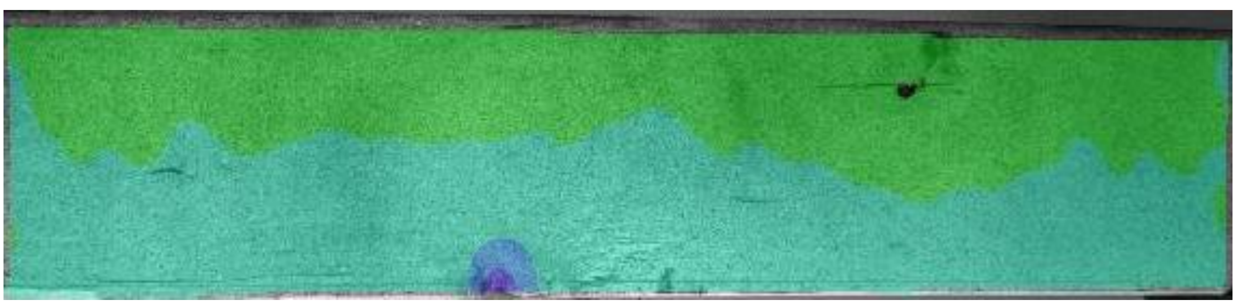

Load: 6000 N

Specimen #5 (Random array of small knots throughout AOI)

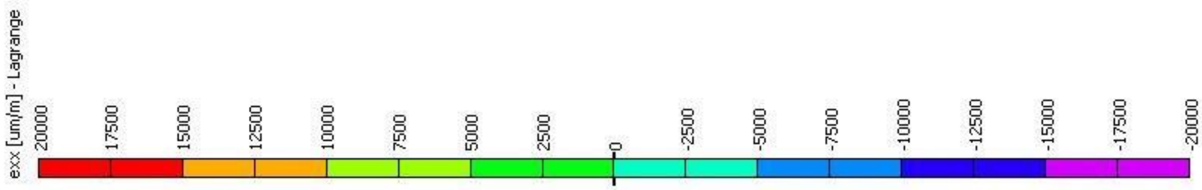

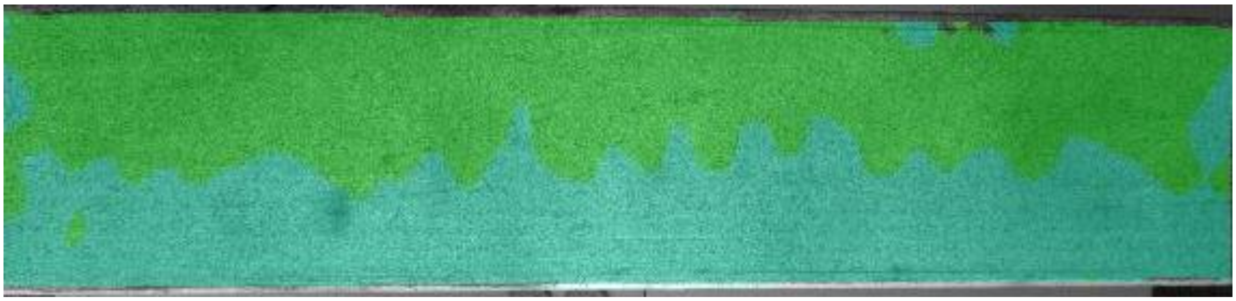

Load: 3000 N

Load: 6000 N

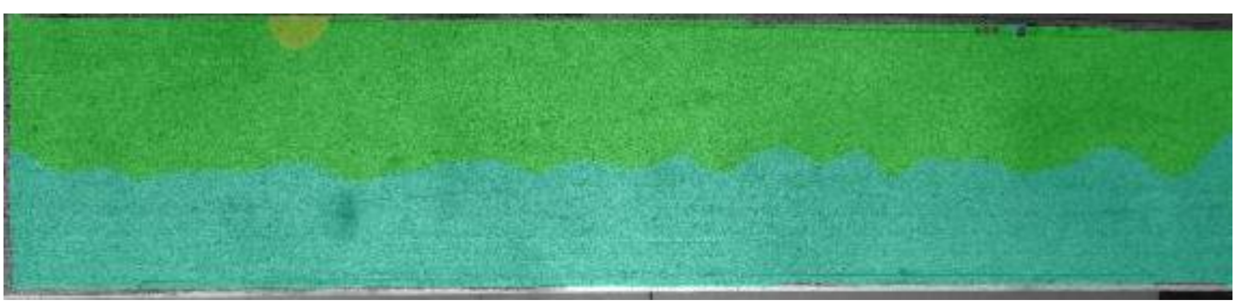

Load: 9000 N

Specimen #6 (Random array of small knots throughout AOI)

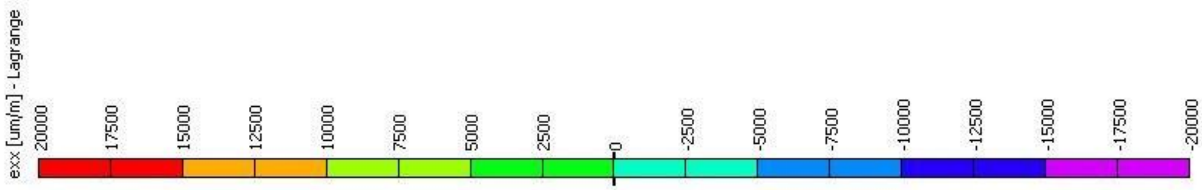

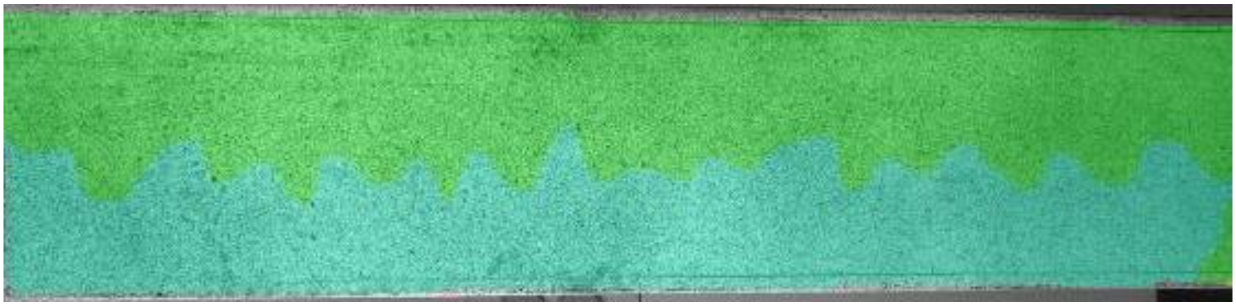

Load: 3000 N

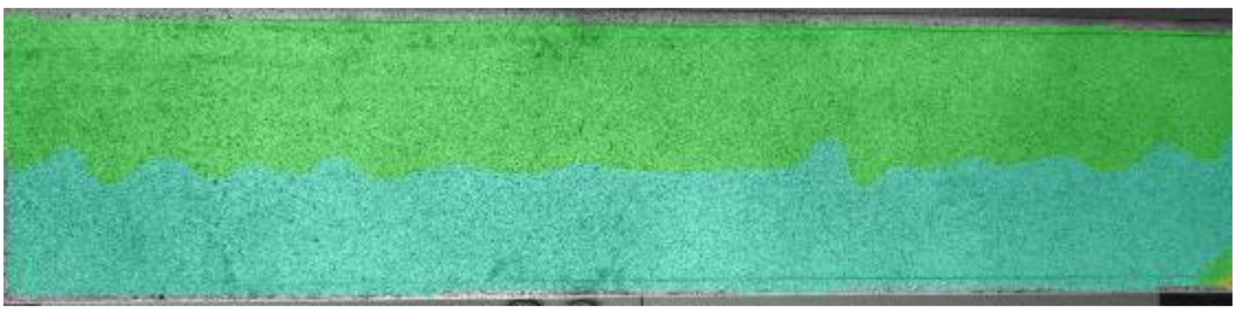

Load: 6000 N

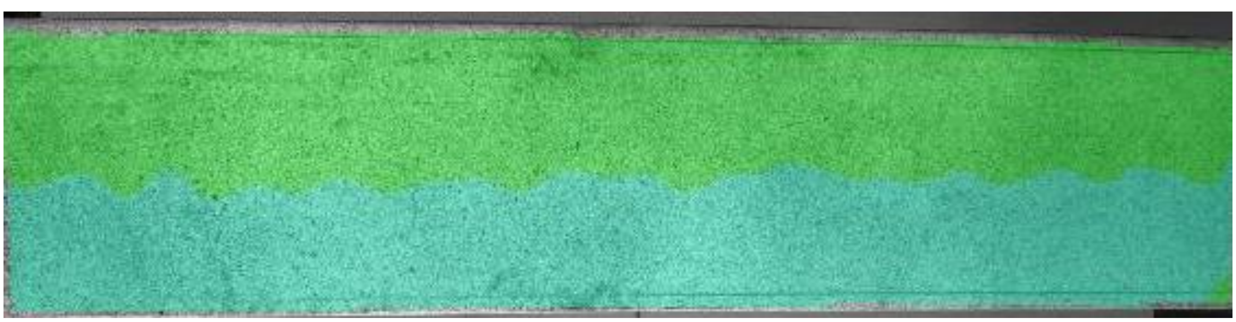

Load: 9000 N

Specimen #7 (Tight knot in compression, loose knot in compression, tight knot in tension)

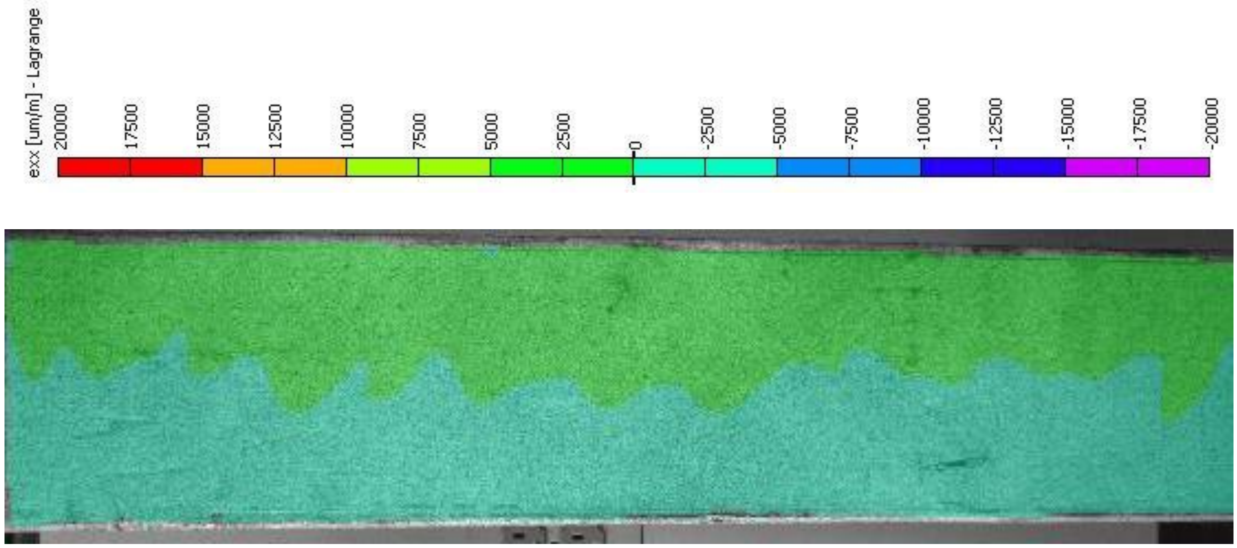

Load: 3000 N

Specimen #8 (Two tight knots in compression, tight knot in tension)

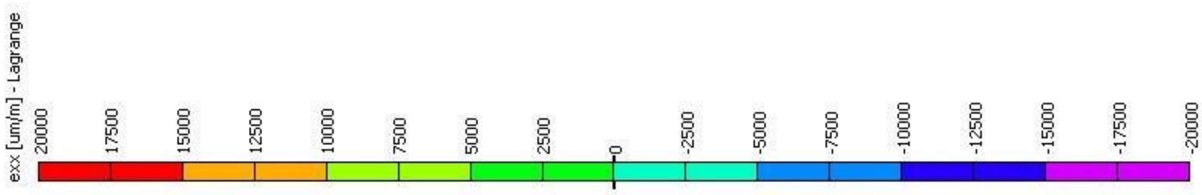

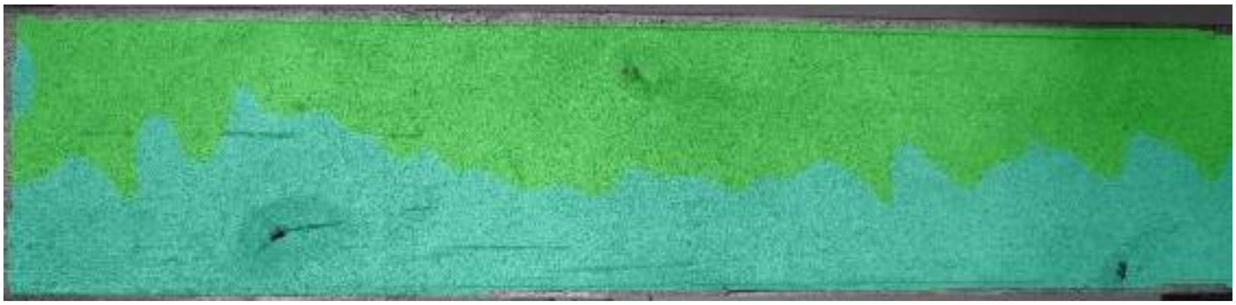

Load: 3000 N

Load: 6000 N

Load: 9000 N

Specimen #9 (Tight knot in compression, tight knot in tension)

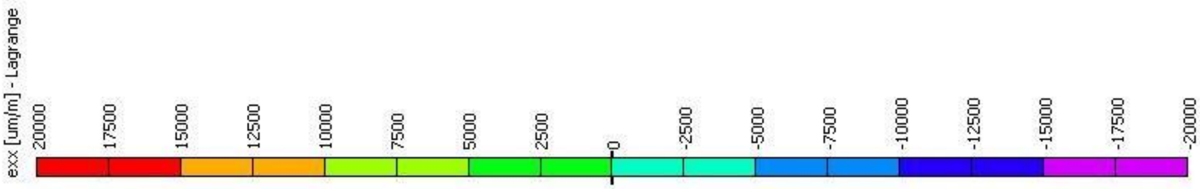

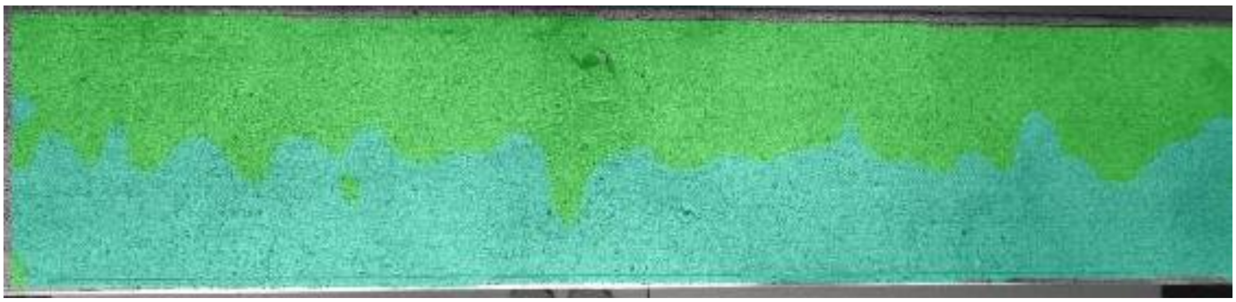

Load: 3000 N

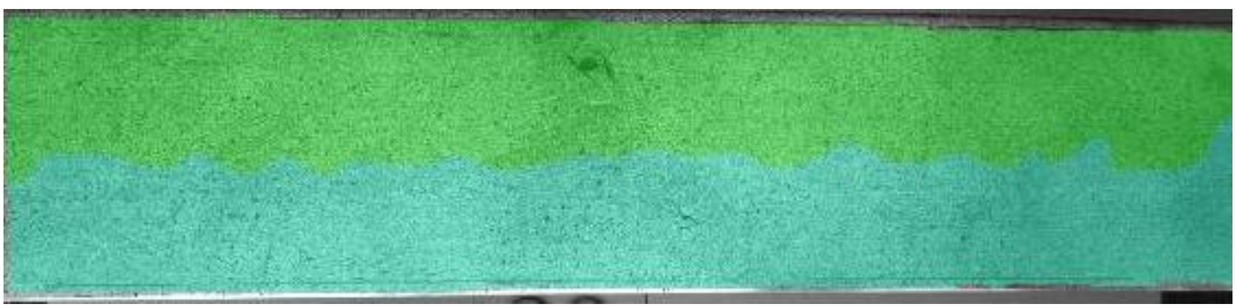

Load: 6000 N

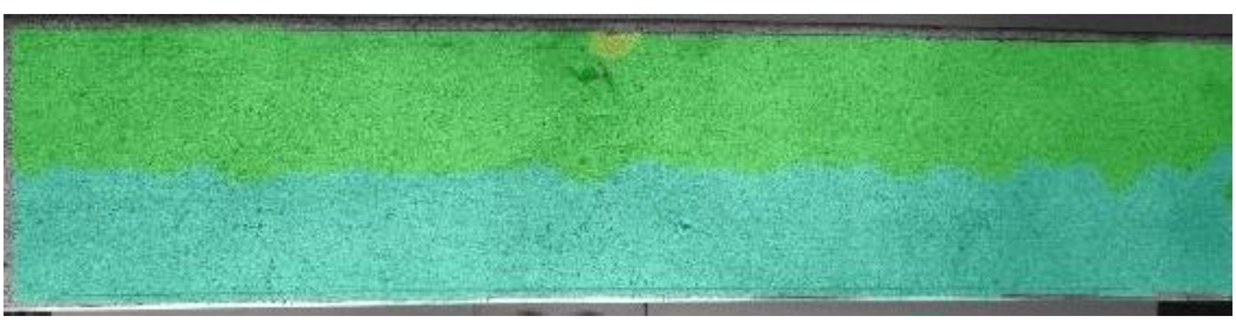

Load: 9000 N

Specimen #10 (Tight knot in compression, tight knot in tension)

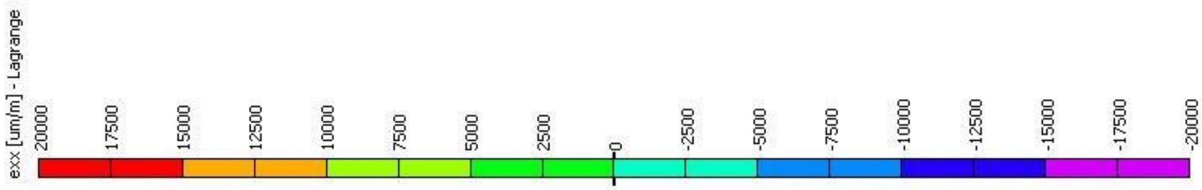

Load: 3000 N

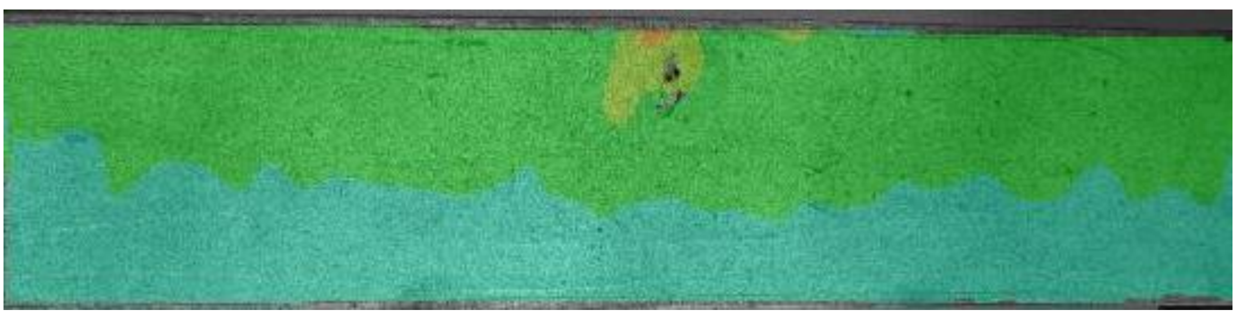

Load: 6000 N

Load: 9000 N

Appendix D
Graphs of Neutral Axis

Specimen #1 (Clear Beam)

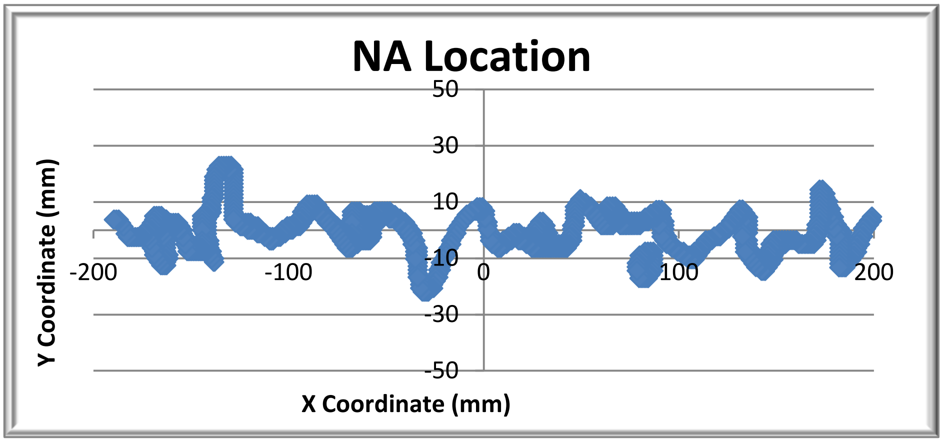

Load: 3000 N

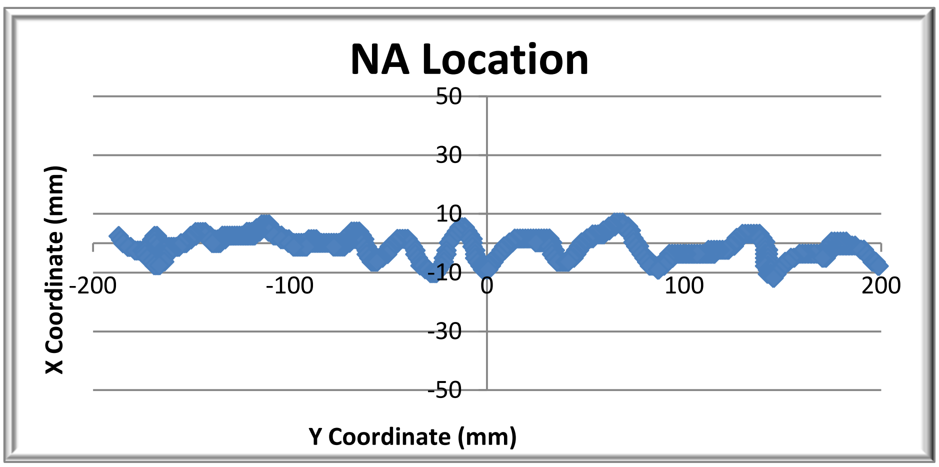

Load: 6000 N

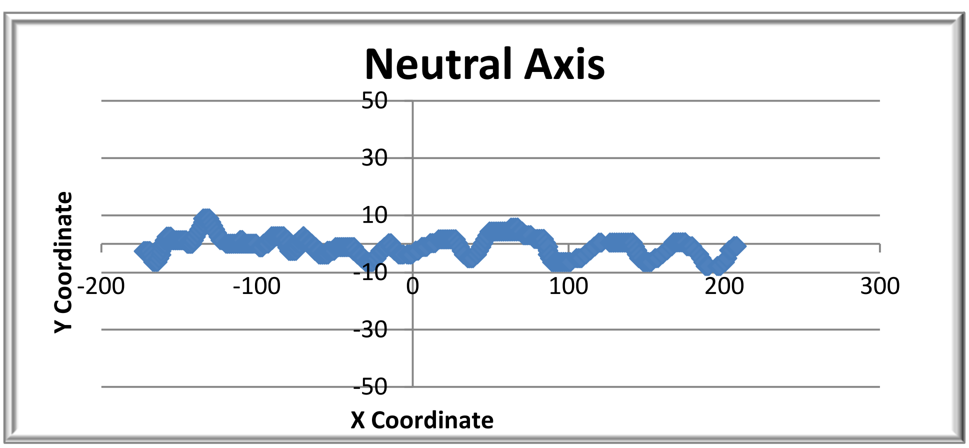

Load: 9000 N

Specimen #2 (Tight group of knots near the center of the beam)

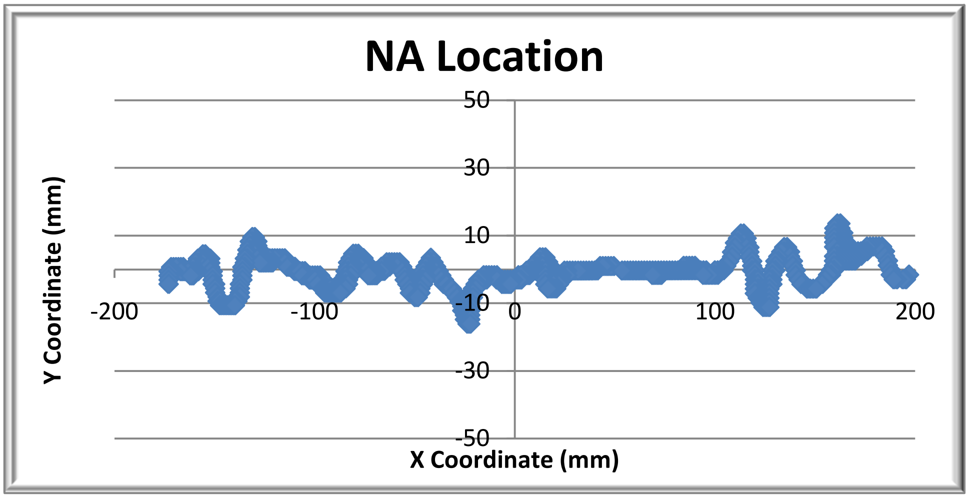

Load: 3000 N

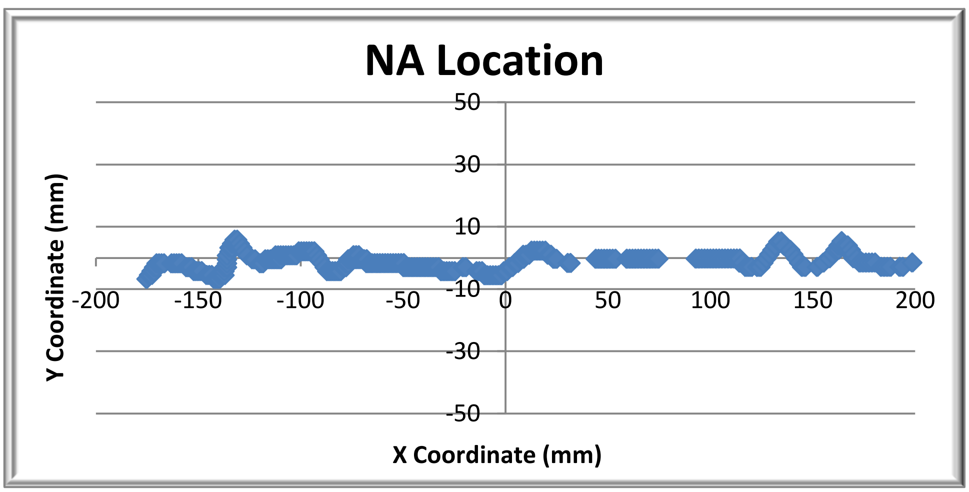

Load: 6000 N

Specimen #3 (Tight knot in compression, loose knot in compression, tight knot in tension)

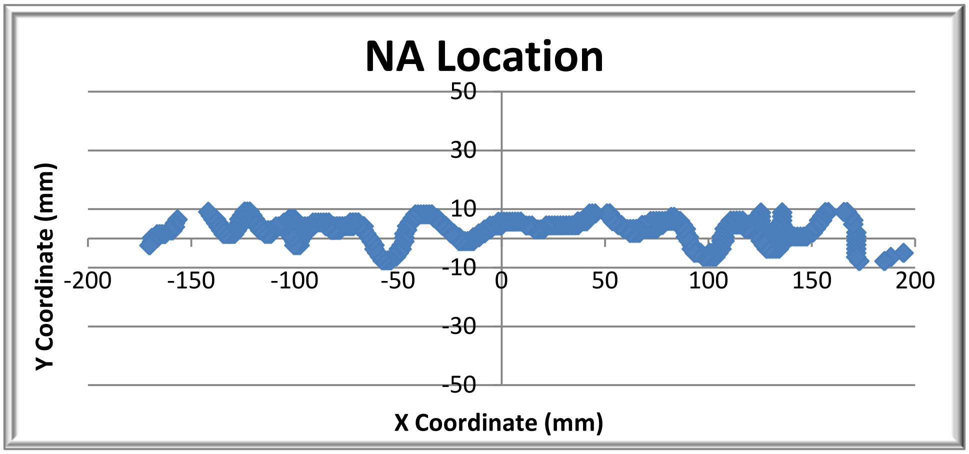

Load: 3000 N

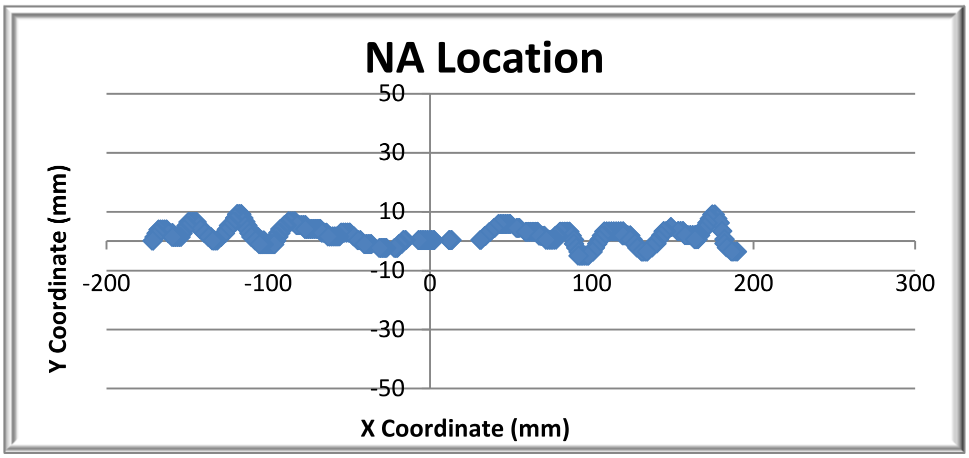

Load: 6000 N

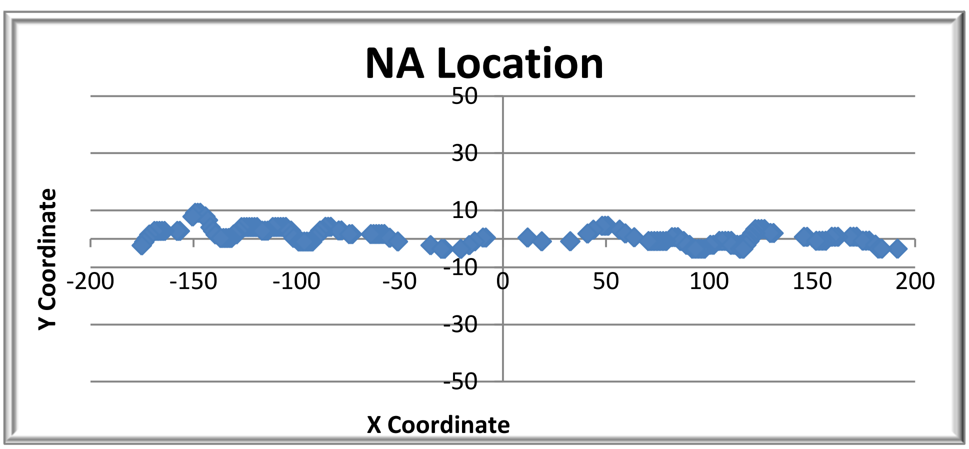

Load: 9000 N

Specimen #4 (Tight knot in compression, tight knot in tension, tight knot near the center)

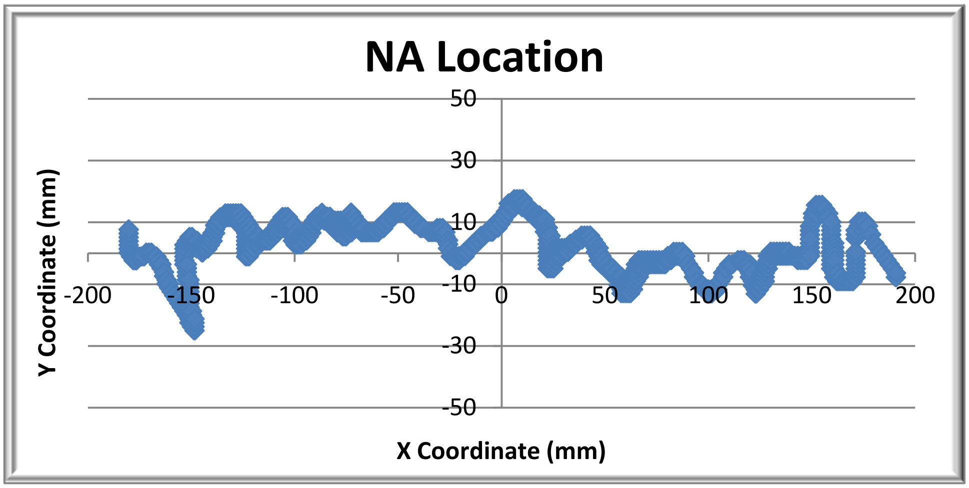

Load: 3000 N

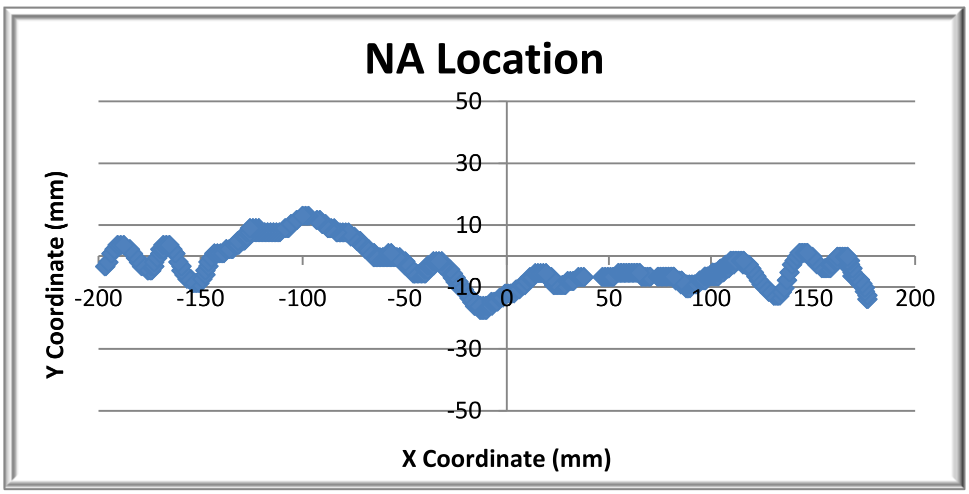

Load: 6000 N

Specimen #5 (Random array of small knots throughout AOI)

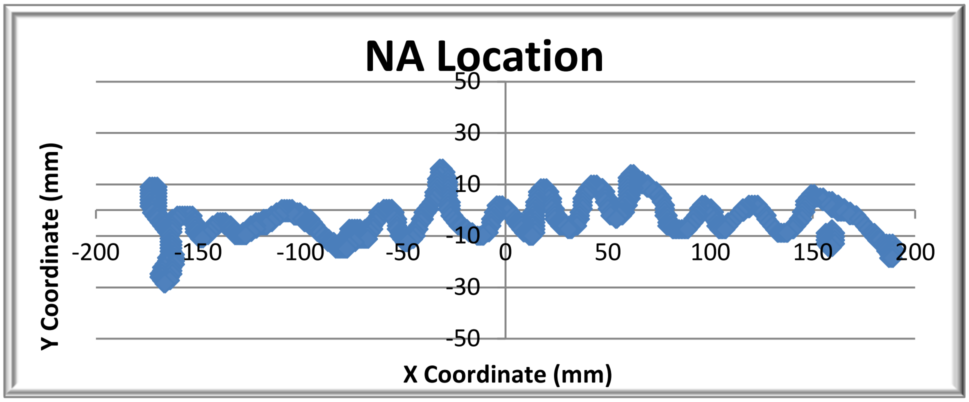

Load: 3000 N

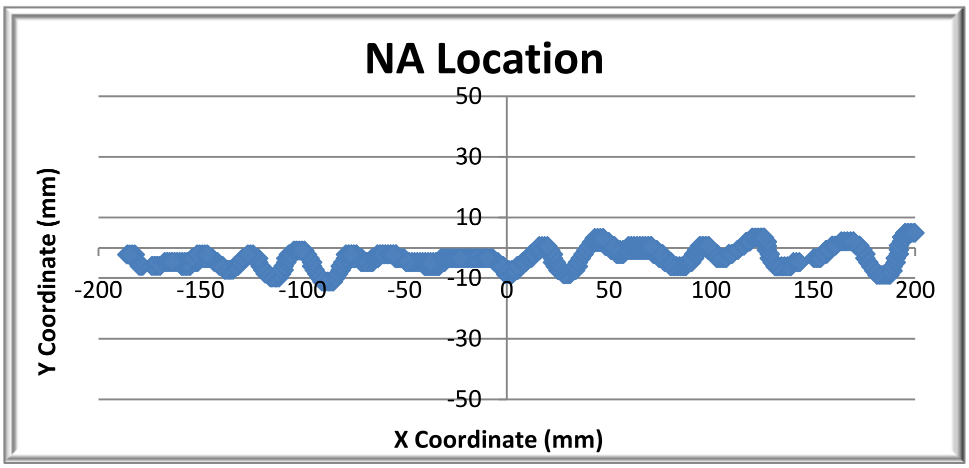

Load: 6000 N

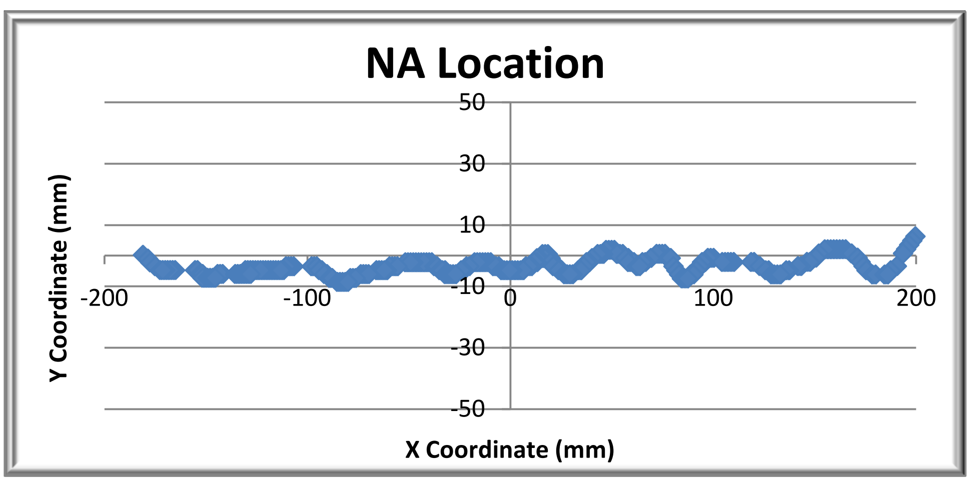

Load: 9000 N

Specimen #6 (Random array of small knots throughout AOI)

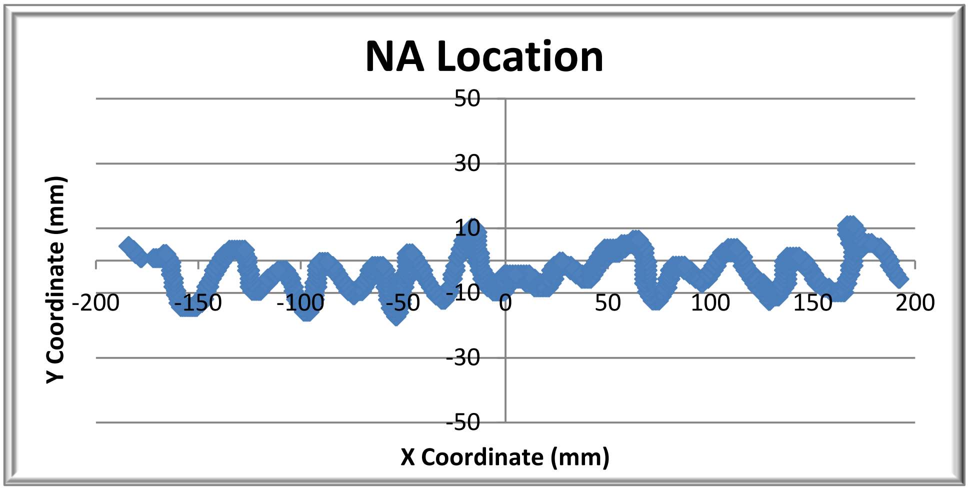

Load: 3000 N

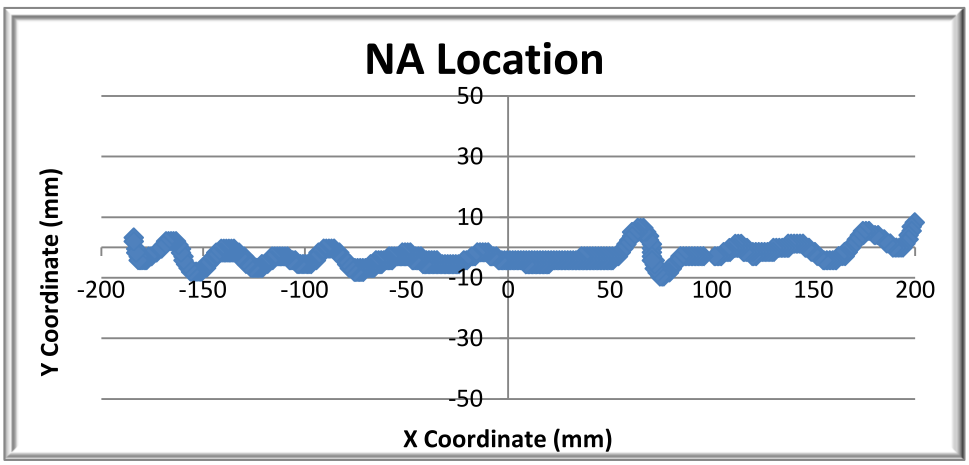

Load: 6000 N

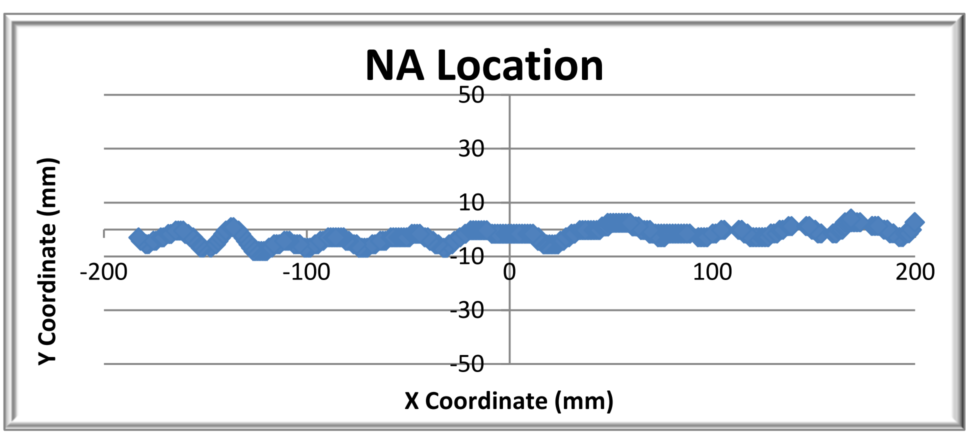

Load: 9000 N

Specimen #7 (Tight knot in compression, loose knot in compression, tight knot in tension)

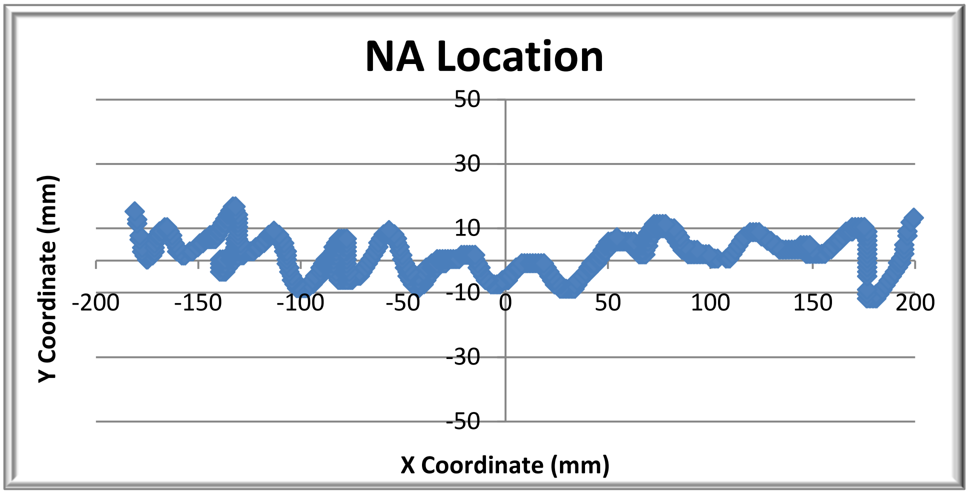

Load: 3000 N

Specimen #8 (Two tight knots in compression, tight knot in tension)

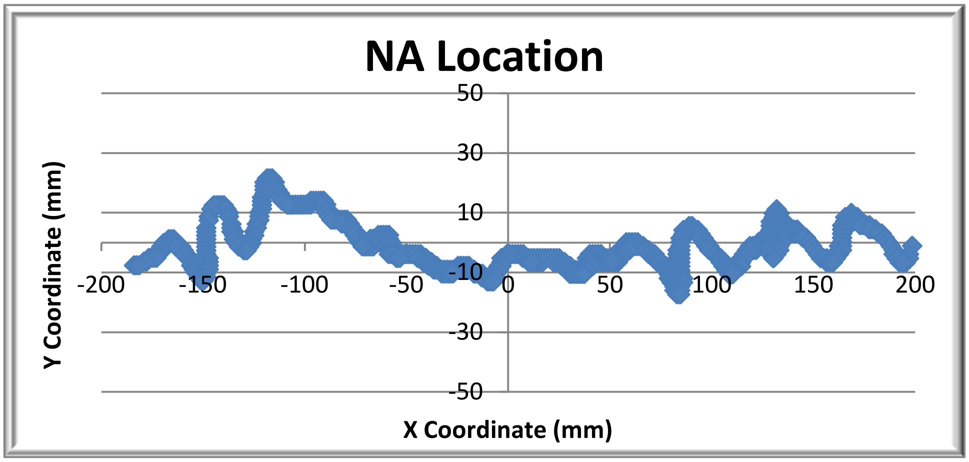

Load: 3000 N

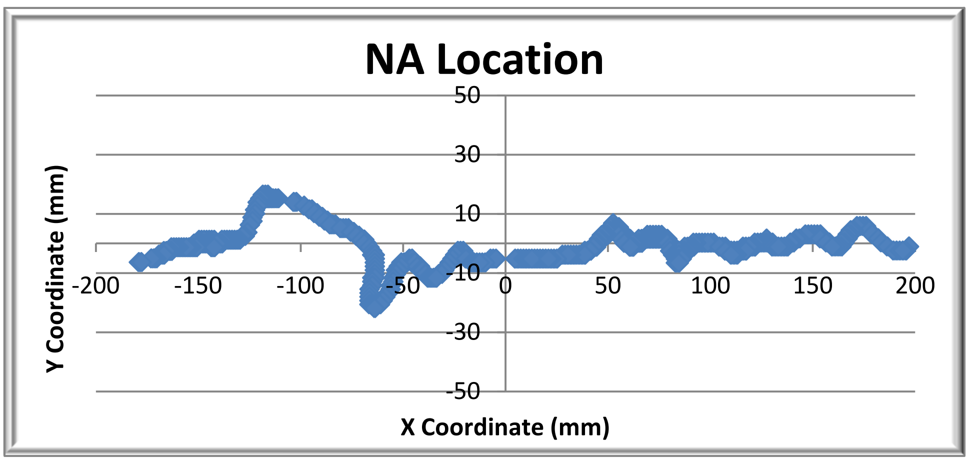

Load: 6000 N

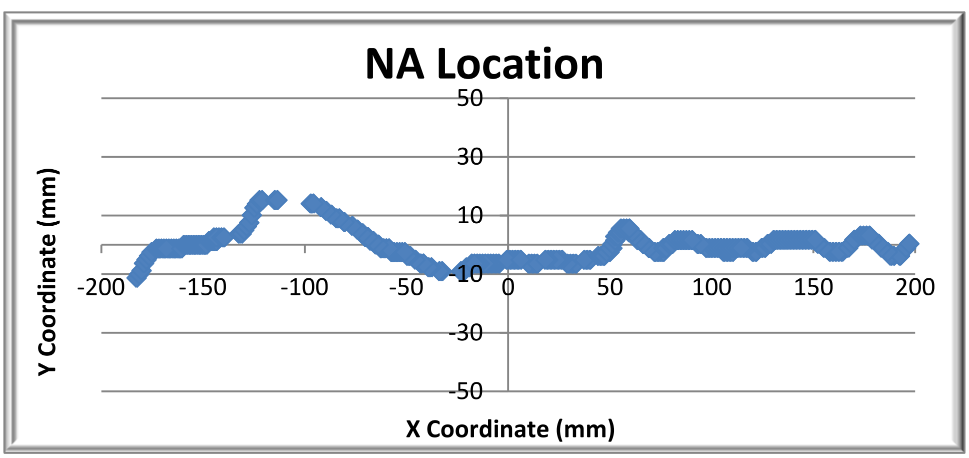

Load: 9000 N

Specimen #9 (Tight knot in compression, tight knot in tension)

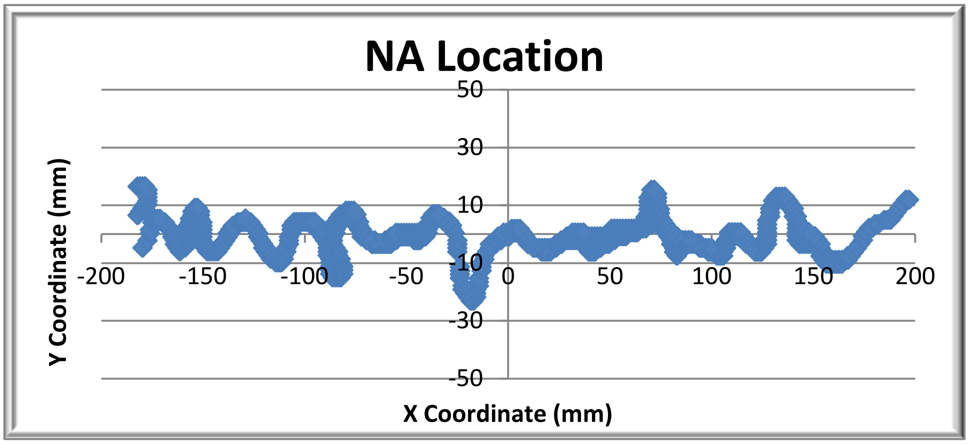

Load: 3000 N

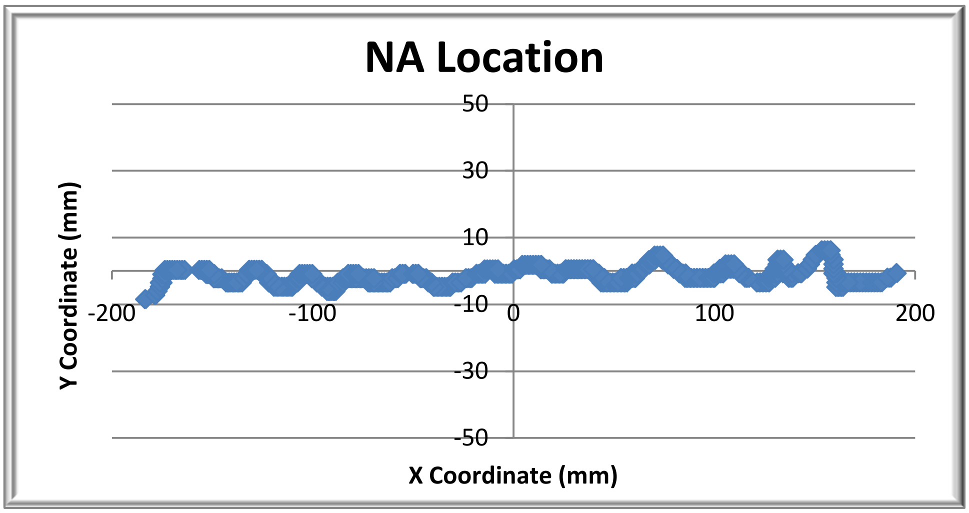

Load: 6000 N

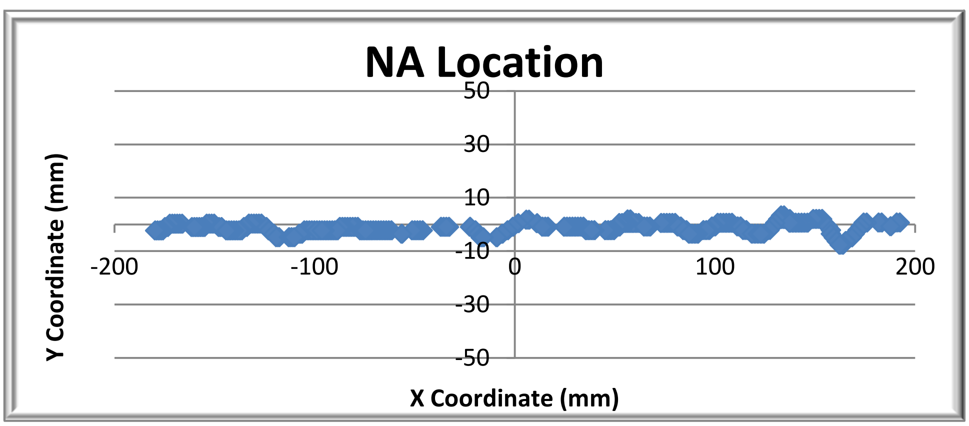

Load: 9000 N

Specimen #10 (Tight knot in compression, tight knot in tension)

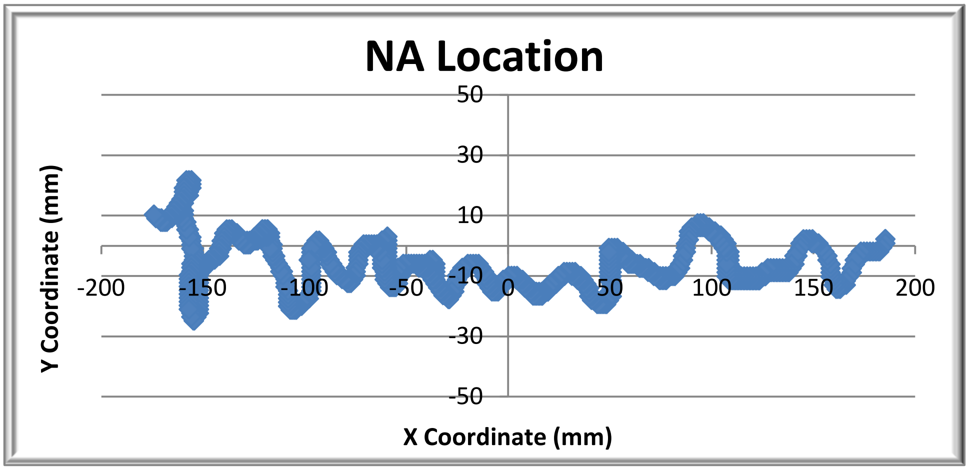

Load: 3000 N

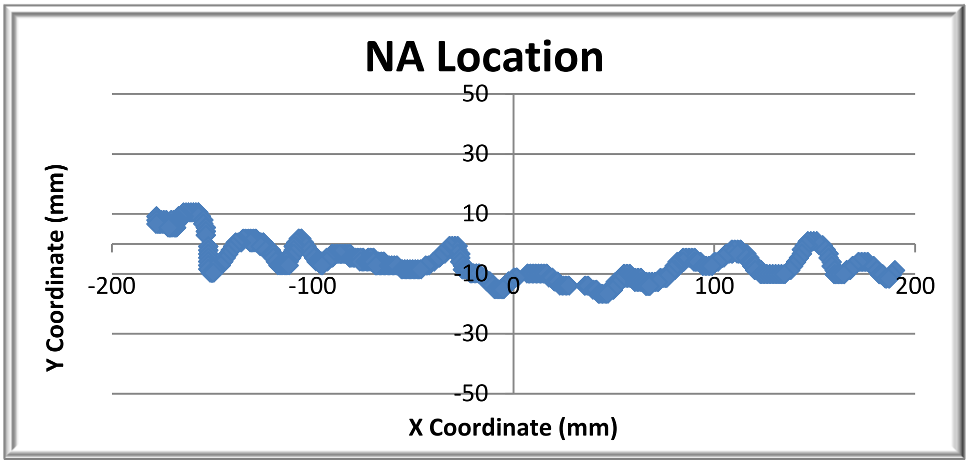

Load: 6000 N

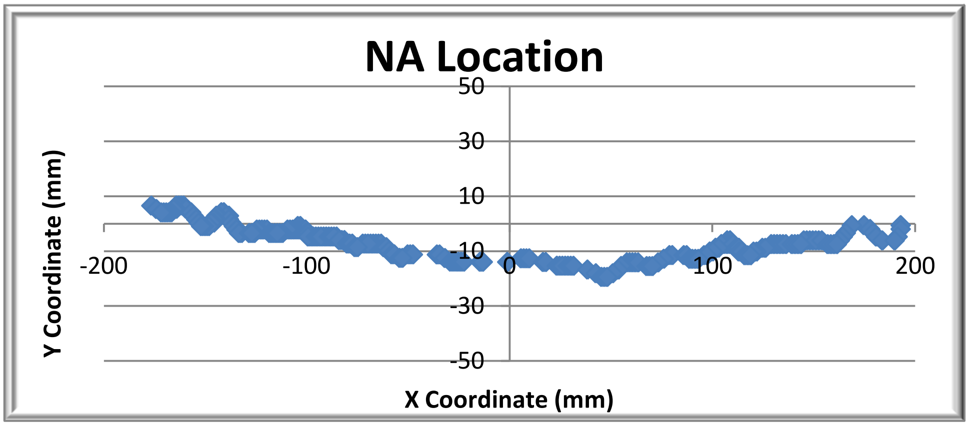

Load: 9000 N